Melanopsin (*opn4*) immunolabelling in the zebrafish (*Danio rerio*) brain

by

Isabel G. Ma

A Thesis Submitted in Partial Fulfillment of the
Requirements for the Degree of

BACHELOR OF SCIENCE (HONOURS)

in the Department of Biology

University of Victoria

We acknowledge and respect the Lək̓ʷəŋən (Songhees and Xʷsepsəm/Esquimalt) Peoples on whose territory the university stands, and the Lək̓ʷəŋən and W̱SÁNEĆ Peoples whose historical relationships with the land continue to this day.

Melanopsin (*opn4*) immunolabelling in the zebrafish (*Danio rerio*) brain

by

Isabel G. Ma

Supervisory Committee

Dr. John S. Taylor, Supervisor
Department of Biology

Dr. Barbara Hawkins, Honours Advisor
Department of Biology

Dr. Terri Lacourse, Honours Advisor
Department of Biology

Abstract

Light is an important signal for vertebrates, not only for image-forming vision, but for non-visual roles including development and physiological responses. Vertebrates detect light using light-sensitive proteins called opsins that are paired with a chromophore. Non-visual opsins are found in a diversity of tissues in vertebrates for both mammals, with the fewest opsins, and ray-finned fishes, with the largest opsin repertoires. Many studies have characterized non-visual opsin mRNA in fish brains, especially in the model zebrafish (*Danio rerio*), and a few studies have delved into the roles of non-visual opsins. Of the non-visual opsins, melanopsin (*opn4*) is the most well-studied. It has been observed in intrinsically photosensitive retinal ganglion cells (ipRGCs), which have various roles, including in the circadian rhythm, pupillary light reflex, and mood. Melanopsin mRNA has been characterized in the zebrafish brain, and melanopsin proteins have been observed in sablefish (*Anoplopoma fimbria*) brains. However, until now, no studies have investigated the expression of melanopsin proteins in zebrafish brains. This study uses immunohistochemistry to show melanopsin proteins in the adult zebrafish brain. Melanopsin occurs in two layers of the optic tectum (the superficial white and grey zone and central zone), the torus longitudinalis, large cells in the paraventricular organ, the torus lateralis, the inferior lobe, and the hypothalamus. Presence of melanopsin proteins in the zebrafish brain is consistent with the hypothesis that the brain is intrinsically light sensitive, and localizing the proteins will help direct future studies designed to test the light-sensitivity hypothesis.

Table of Contents

List of Figures

List of Tables

Acknowledgements

I would like to thank people who were vital to this project, as well as those whose feedback, advice, and demonstrations helped me learn and improve.

Dr. John S. Taylor has been a wonderful mentor sharing inspiration, guidance, and support through the entire project. Dr. Takeshi Yoshimatsu from Washington University in St. Louis made this project possible by gifting me zebrafish samples. Golden Eagle Sablefish gifted sablefish brains. Dr. Bob Chow's generosity was a huge help, including advice, showing me how to use his confocal microscope, and letting me use his cryostat microtome and confocal microscope.

Dr. Bridget Ryan and Tariq Nashmi showed me how to do immunolabelling and use the cryostat, respectively. Dr. Kerry Delaney gave advice, showed me how to use the oil lens on the confocal, and worked with me to try to determine cell types through morphology.

Dr. Niloufar Mokaraisl shared advice to help me get started with the workflow and oriented to where reagents were. Additionally, Niloufar Mokariasl and Hayley Barnes's past work inspired this project. Sammy Weisner Novak shared his wealth of histological and imaging information to help me troubleshoot and improve my embedding and sectioning protocols. Drs. Craig Brown and Gautam Awatramani shared insights and advice. Drs. Barbara Hawkins and Terri Lacourse informed me about the honours program and always enthusiastically answered my questions.

I acknowledge the support of the Natural Sciences and Engineering Research Council of Canada (NSERC) (funding reference number USRA - 603029 - 2025) for an NSERC URSA grant that helped this project begin in the summer, giving me time to learn the techniques and start my Honours with a working protocol so I was able to get results. This work was also supported by an NSERC Discovery Grant to Dr. John Taylor.

List of Abbreviations

A: anterior

ATN: anterior tuberal nucleus

CB: cerebellum

Some studies refer to it as the corpus cerebelli (CCe)

CZ: central zone of the optic tectum

It contains multiple layers, in order from more dorsal (closer to superficial white and grey zone) to more ventral (closer to periventricular grey zone), they are: stratum fibrosum et griseum superficiale (SFGS) (which itself has multiple layers), stratum griseum centrale (SGC), and the stratum album centrale (SAC)

D: dorsal

DV: diencephalic ventricle

GCL: ganglion cell layer

GPCR: G-protein coupled receptor

HT: hypothalamus

IL: inferior lobe

INL: inner nuclear layer

IPL: inner plexiform layer

KLH: keyhole limpet hemocyanin

L: left side of fish

MB: mamillary body

Some studies refer to it as the corpus mamillare (CM)

MO: medulla oblongata

OB: olfactory bulb

OCT: optimal cutting temperature compound

ON: optic nerve

ONL: outer nuclear layer

OPL: outer plexiform layer

OT: optic tectum

Some studies refer to it as the tectum opticum (TeO)

P: posterior

PBS: phosphate buffered saline

PFA: paraformaldehyde

PGZ: periventricular grey zone of the optic tectum

Some studies refer to it as the stratum periventriculare (SPV)

PMT: pretecto-mammillary tract

PR: photoreceptors

PT: posterior tuberculum

PVO: paraventricular organ

R: right side of fish

RGC: retinal ganglion cell

SWGZ: superficial white and grey zone of the optic tectum

It consists of two layers, the stratum marginale (SM) and stratum opticum (SO). Some studies just refer to it as the superficial layer.

TC: tectal commissure

Tel: telencephalon

TH: thalamus

TL: torus longitudinalis

TLa: torus lateralis (also called lateral torus)

TV: tectal ventricle

V: ventral

VC: valvula cerebelli

VOT: ventrolateral optic tract

ZL: zona limitans

Introduction

Light sensitivity occurs across the tree of life. Bacteria are capable of phototaxis (Taylor *et al*., 1999), plants regulate flowering timing using light (Kami *et al*., 2010), fungal growth and stress responses are impacted by light (Yu and Fischer, 2018), and vision has evolved multiple times leading to a diversity of animal visual systems (Fernald, 2000). Animals sense light using opsins, a family of 7-transmembrane G-protein coupled receptors (GPCRs) with a characteristic lysine residue in the ligand-binding pocket that enables them to pair with a chromophore called retinal (Terakita, 2005). When light of the appropriate wavelength hits the complex, 11-*cis*-retinal changes into all-*trans*-retinal and initiates an opsin-mediated G-protein signal cascade (Terakita, 2005). Some opsins, such as rhodopsin (*rho*), release all-*trans*-retinal, which is then converted back to 11-*cis*-retinal in the "visual cycle", which involves photoisomerases such as retinal G-protein receptor (RGR) (also a member of the opsin family) (Terakita, 2005; Sato and Kefalov, 2024) in the retinal pigmented epithelium. Other opsins, such as melanopsin (*opn4*), are bistable, binding and converting retinal between both forms by reacting to different wavelengths of light (Davies *et al*., 2011; Upton *et al*., 2021). Different opsins tune their chromophore to absorb different wavelengths of light, and different opsins bind different G-proteins, for example rhodopsin activates the G-protein transducin (G_T), and melanopsin pairs with G_q (Terakita, 2005; Upton *et al*., 2021).

The most studied vertebrate opsins are those involved in vision, loosely termed "visual opsins", which are densely packed in the outer segments of rod and cone photoreceptor cells (Purves, 2001). When activated by light, vertebrate visual opsins lead to rod and cone hyperpolarization (Purves, 2001). This seems counterintuitive as most vertebrate neurons depolarize and fire an "all-or-none" action potential upon activation, but the vertebrate retina is an unusual neural structure that processes "graded potentials", retaining details from subtle shifts in voltage until sending signals to the brain (Purves, 2001). The vertebrate visual opsins include rod opsins, rhodopsin (*rho*), and various cone opsins, including long-wavelength sensitive opsins (*lws*, detect red), medium-wavelength sensitive opsins (*mws*, detect green), short-wavelength sensitive opsins (sws blue), and some species have UV-sensing opsins (Terakita, 2005). Different vertebrate taxa have varying numbers of opsins. Mammals have the fewest visual opsins, with one rod opsin, *rho* (*opn2* family), and two cone opsins (*opn1* family), *lws* (red), and *sws* (blue), making them dichromatic. Old World monkeys, apes, and humans have a third cone opsin (a

second, modified *lws*) (Jacobs, 2008). Ray-finned fish (Actinopterygii) have a much larger array of visual opsins than other vertebrates, for example zebrafish (*Danio rerio*) have ten visual opsins (Rennison *et al*., 2012).

Visual opsins are only a fraction of the full opsin repertoire. Vertebrates also have a diversity of "non-visual" opsins, including other members of the *opn1* family (such as pinopsin, parapinopsins, parietopsin, and vertebrate ancient opsins), encephalopsins (*opn3* and teleost multi-tissue (TMT) opsins), melanopsins (*opn4*), and neuropsins (*opn5, opn6*, *opn7*, *opn8*, *opn9*) (Terakita, 2005; Davies *et al*., 2015; Beaudry *et al*., 2017; Andrabi *et al*., 2023; Gyoja *et al*., 2025). Two tissues commonly studied for light sensitivity are the retina and pineal gland. The mammalian retina has intrinsically photosensitive retinal ganglion cells (ipRGCs) that express melanopsin and regulate circadian rhythm, pupillary constriction, photoreceptor sensitivity, development, and mood (Raja *et al*., 2023; Meng *et al*., 2025). Non-mammalian vertebrates have light-sensitive cells in their pineal gland that express opsins (Ekstrom and Meissl, 2003). For example, the pineal gland is involved in regulating African clawed frog (*Xenopus laevis*) skin pigmentation changes (Bertolesi *et al*., 2020). Opsins in fish also have a variety of functions, including circadian rhythm entrainment and skin colour changes, and some opsins show rhythmic expression patterns (Matos-Cruz *et al*., 2011; Cooper *et al*., 2025). For example, melanopsin expression can vary depending on photoperiod length (Matos-Cruz *et al*., 2011) and temperature (Sua-Cespedes *et al*., 2025).

Interestingly, despite the many functions tied to non-visual opsins in mammals (Shi *et al*., 2025), mammals have the fewest opsins among vertebrates, while ray-finned fish have the most opsins (Beaudry *et al*., 2017; Gyoja *et al*., 2025). This difference can be correlated with evolutionary events. Mammals went through a nocturnal bottleneck leading to loss of opsins (Borges *et al*., 2018). In contrast, ray-finned fish gained opsins through a whole genome duplication around 335-404 million years ago and subsequent tandem duplications (Hoegg *et al*., 2004; Rennison *et al*., 2012; Beaudry *et al*., 2017). One hypothesis for the retention of these extra opsins for a long time is that they serve important roles, which may be subsets of roles that the ancestral opsins played, such as was found for the cichlid visual opsins (Spady *et al*., 2006). If multiple opsins in fish play the role of one opsin in their ancestors, perhaps one opsin in mammals has consolidated functions from multiple opsins. Studying opsins in fish could reveal

nuanced insights into the evolution and roles of opsins and non-visual photoreception in vertebrates.

There is a growing body of evidence demonstrating expression of non-visual opsins in a variety of brain regions, not just the pineal gland. Opsin gene expression (*i.e*., mRNA, transcripts) has been found in various regions of human brains (Moraes e*t al*., 2021) and the *Xenopus laevis* brain (Provencio *et al*., 1998). There is a wealth of studies characterizing opsin gene expression in teleost brains, including exorhodopsin and melanopsin in Atlantic halibut larvae (*Hippoglossus hippoglossus*) (Eilertsen *et al*., 2014), VA opsin and melanopsin in Atlantic salmon (*Salmo salar*) (Philp *et al*., 2000; Sandbakken *et al*., 2012), melanopsin in Atlantic cod (*Gadus morhua*) (Drivenes *et al*., 2003) and numerous opsins in the zebrafish optic tectum, thalamus, hypothalamus, and more (Bellingham *et al*., 2002; Davies *et al*., 2015; Hang *et al*., 2016; Dekens *et al*., 2022). Some studies in zebrafish, a model teleost, have demonstrated light reactivity in cultured cells, such as neuro-2a cells transfected with zebrafish melanopsin and cultured zebrafish tissues, including skin, liver, gut, and brain cells (Davies *et al*., 2011; Davies *et al*., 2015). Wada *et al*. (2018) used two-photon calcium imaging to demonstrate colour opponency in the pineal organ arising from one opsin protein, bistable parapinopsin. Dekens *et al*. (2022) observed reduction in larval locomotor behaviour during the waking period after knocking out two of the five zebrafish melanopsins, *opn4m2* and *opn4x2*. Despite the prevalence of melanopsins in opsin related studies (Andrabi *et al*., 2023), there seem to be no publications to date on melanopsin protein localization in zebrafish brains. While mRNA tends to correlate with presence of proteins, mRNA is not a perfect indication of protein expression due to intermediate regulatory steps (Buccitelli and Selbach, 2020) and does not show where the proteins ultimately localize. Two studies have observed melanopsin proteins in various regions of sablefish (*Anoplopoma fimbria*) brains, including the optic tectum (Barnes, 2022; Mokariasl, 2024), however sablefish are a poor model due to their large size and slow growth (Mason *et al*., 1983). For example, to establish a line of transgenic sablefish (*e.g.,* knock out a gene of interest, add GFP to a specific cell type), embryo injection protocols would need to be developed; CRISPR guide RNA sequences (or other gene-editing protocols) would need to be created; an enormous, dark, chilled, marine fish facility would need to be designed and built to house the sablefish; and researchers would need to wait years for each generation to mature.

The goal of my honours work was to address this gap in knowledge about melanopsin proteins in the zebrafish brain by characterizing the location of melanopsins using antibody immunolabelling, with a focus on the optic tectum. To do so, I utilized melanopsin specific antibodies, OPN4L (anti-*opn4m2*) and pas350 (anti-*opn4m1*, *opn4m2*, and *opn4m3*) to immunolabel juvenile and adult zebrafish brain sections. I found distinct OPN4L labelling in the optic tectum and in two distinct cells in the paraventricular organ, as well as pas350 labelling in the optic tectum, torus longitudinalis, torus lateralis, and inferior lobe.

While presence of opsins leads to hypotheses about light sensing, it does not demonstrate light sensitivity. For example, some opsins respond to other stimuli such as heat (Feuda *et al*., 2022). Even opsins that can respond to light might not do so in all tissues, for example, while the mouse pineal has rhodopsin, it lacks the machinery to reset retinal, so seems unlikely to be involved in photoreception (Kramm *et al*., 1993). As important model vertebrates, numerous methods have been developed for testing the roles of proteins in zebrafish, such as live calcium imaging in transparent *casper* zebrafish (White *et al*., 2008; Wada *et al*., 2018; Mu *et al*., 2019), and gene knockouts with behavioural assays (Dekens *et al*., 2022). Identifying melanopsin protein localization will help guide future studies using these tools to identify the roles of melanopsin in other brain regions by focusing efforts onto specific regions and cell types within the brain.

Materials and Methods

Alignment and BLAST Searches

The OPN4L and pas350 primary antibodies were created through raising antibodies to a conjugated protein made of a synthetic peptide, which matched a region of the zebrafish melanopsin sequences, attached to keyhole limpet hemocyanin (KLH). To check which of the melanopsins OPN4L and pas350 bind, the synthetic peptide sequences were obtained from ThermoFisher's website and Davies *et al*. (2011), respectively. OPN4L's antibody binds to a peptide corresponding to positions 255-288 of "DANRE opn4l" and the sequence was extracted from UniProt Q1JPS6-1.

The amino acid versions of the five zebrafish melanopsin genes indicated by Beaudry *et al*. (2017) and melanopsin sequences found by searching for melanopsin in zebrafish on NCBI's

Gene database were obtained from NCBI (Table 1). Amino acid sequences for the five sablefish melanopsins were obtained from Barnes (2022). These sequences were aligned to one another to generate a multiple sequence alignment in BioEdit (version 7.7.1) using the inbuilt ClustalW (version 1.4). These sequences were compared to one another, as well as information from the Zebrafish Information Network (ZFIN), to identify the alternative names used for each of the five melanopsins. The potential for antibody binding was assessed by manually aligning the antibody immunogen sequences to the multiple sequence alignment of melanopsins.

Table 1. NCBI accessions of the collected zebrafish (*Danio rerio*) melanopsin sequences.

Gene	Accession
opn4m1	ALG92568.1
opn4m2	ALG92569.1
opn4m3	ALG92570.1
opn4x1	ALG92571.1
opn4x2	ALG92572.1
opn4.1	NP_840074.2
opn4b	NP_001245153.1
opn4a	XP_073775997.1

To check for nonspecific binding, the immunogen sequence for OPN4L was input as the query to multiple NCBI BLAST searches against zebrafish and sablefish using the default settings. These included blastp searches in the nr and refseq_protein databases and tblastn searches in the core_nt and nt databases. To search for more distant matches, another set of tblastn searchers were done with a word size of 2 and gap costs lowered to Existence = 9, Extention =1, with the refseq_genomes databases (these settings will be referred to as “lenient”). Reducing the word size and decreasing the gap size allows the search to find more distantly related proteins and searching the whole genome includes non-annotated sequences. Lenient searches were done on the whole antigen sequence, the first 17 amino acids, and the last 17 amino acids to search for partial matches. Additionally, I used discontiguous megablast (allows mismatches) to search for any matches to the only two available non-patent related sequences of keyhole limpet hemocyanin (*Megathura crenulata* KLH1 Accession AJ698341.2, and KLH2

Accession AJ698342.1) in the zebrafish and sablefish. Details about the search results can be found in Appendix A.

Samples

Zebrafish (*Danio rerio*) samples were a gift from Dr. Takeshi Yoshimatsu at Washington University in St Louis (WashU). They were cared for in accordance with AUP#AE-25-013 and arrived at UVic as fixed samples of whole larvae, whole heads, or isolated brains. The zebrafish samples included the head of a wild type (AB*) juvenile, two wild-type adult brains (3 months old), two adult *casper* brains (no skin pigmentation (White *et al*., 2008); 6 months old), and three 10 days post fertilization (dpf) *casper* larvae. Two samples of transgenic zebrafish under wild-type backgrounds (*i.e.*, not transparent) were also received, one was the head of a juvenile transgenic zebrafish with red fluorescent protein (RFP) expressed by a myosin promotor, and the other was one brain of a juvenile transgenic zebrafish with mCherry expressed by a retinal ganglion cell (RGC) specific promotor (Tg(*isl2b*:QF2,QUAS:loxP-mCherry-loxP-memGCaMP8m)), which was referred to as "RGC labelled" throughout this thesis. Juvenile and adult zebrafish were housed at WashU with a light cycle of 14 hours light and 10 hours dark (light on at 7:30 am, light off 9:30 pm central time). Larval zebrafish were housed in an incubator with the same light cycle as adults and juveniles from 0-5 dpf, then were moved to a different incubator with a cycle of 14 hours light and 10 hours dark that was offset by 3.5 hours (light on 11:00 am, off 1:00 am central time).

Casper zebrafish were included to check whether melanopsin expression differed between the transparent line and the wild types to aid future studies on melanopsins that use transgenic *casper* zebrafish for imaging. Transparent zebrafish, whether through application of phenylthiourea (PTU) or through crossbreeding, lack pigment cells to obstruct imaging lasers, leading to better results from live imaging (White *et al*., 2008; Antinucci and Hindges, 2016; Shen *et al*., 2025).

A juvenile sablefish brain (*Anoplopoma fimbria*) was gifted by Golden Eagle Sablefish.

Reagents

10X Phosphate buffered saline (PBS) was prepared in the lab using 1.37 M NaCl, 0.027 M KCl, 0.1 M Na_2HPO_4, and 0.018 M KH_2PO_4. 1X PBS was prepared by diluting the lab-made 10X PBS.

4% Paraformaldehyde (PFA) was prepared in a fume hood using 30 mL 1X PBS, and 10 mL 16% PFA (Electron Microscopy Sciences Cat. No. 15710 Lot No. 250620-50).

Primary antibodies and secondary antibodies used in this study are detailed in Table 2. OPN4L was developed against a synthetic immunogen created from conjugating keyhole limpet hemocyanin (KLH) peptide to amino acids 255-288 from the central region of zebrafish *opn4m2*. pas350 was also created by conjugating an *opn4m*-based peptide to KLH. GFAP labels glial cells in the brain and Muller glia in the retina (Bernardos and Raymond, 2006). Because the intrinsic mCherry fluorescence was quenched during the fixation process, the RGC labelled brains needed to be labelled with an anti-mCherry antibody to visualize the retinal ganglion cells. The anti-dsRed and anti-RFP antibodies were used for this purpose.

Table 2. Antibodies used in this study.

Antibody	Type	Host	Antigen	Origin	Cat. No. (Lot No.)	RRID	Dilution used	Comments
OPN4L	Primary, polyclonal	rabbit	Synthetic peptide from zebrafish *opn4m2* conjugated to keyhole limpet hemocyanin (KLH)	Invitrogen	PA5-72273 (79560889)	AB_2718127	1:250 to 1:10,000	0.5 mg/mL
pas350	Primary, polyclonal	rabbit	Synthetic peptide from zebrafish *opn4m1*, *opn4m2*, and *opn4m3* conjugated to KLH	Davies *et al*. (2011)	N/A	unknown	1:250 to 1:500	Provided by Wayne Davies and Stephen Hughes, authors in Davies *et al*. (2011). Mixed 1:1 with glycerol.
GFAP	Primary, polyclonal	chicken	GFAP	Invitrogen	PA1-10004 (XI3685001)	AB_1074620	1:500 to 1:2000; usually 1:1600	Mixed 1:1 with glycerol
anti-dsRed	Primary, polyclonal	rabbit	dsRed	Clontech	632496 (unknown)	AB_10013483	1:250	Gifted by Dr. Bob Chow. Mixed 1:1 with glycerol.

Antibody	Type	Host	Antigen	Origin	Cat. No. (Lot No.)	RRID	Dilution used	Comments
anti-RFP	Primary, monoclonal	rat	RFP	ChromoTek	5F8 (aliquot A: 104272; aliquot B: 90228002AB-14)	AB_2336064	1:250	Gifted by Dr. Bob Chow
Alexa 555	Secondary	donkey	rabbit IgG (H+L)	Invitrogen	A31572 (2339822)	AB 162543	1:500 to 1:1000	2 mg/mL
Alexa 488	Secondary	goat	chicken IgY (H+L)	Invitrogen	A11039 (2420700)	AB_2534096	1:500	2 mg/mL. Mixed 1:1 with glycerol.
Alexa 555 for anti-dsRed	Secondary	donkey	rabbit antibodies	Invitrogen	A-31572 (unknown)	AB_162543	1:500	Gifted by Dr. Bob Chow
Alexa 555 for anti-RFP	Secondary	donkey	rat antibodies	Invitrogen	48270 (unknown)	AB_2896336	1:500	Gifted by Dr. Bob Chow

Sample Fixation, Cryoprotecting, and Embedding

The juvenile wild-type head and the transgenic (Tg(*mylpfa*:RFP)) juvenile zebrafish head were fixed overnight at 4°C in 4% PFA, washed 3 times in 1X PBS for 10 minutes each, then incubated with cryoprotectant, 1X PBS with 30% sucrose, for 48 hours at in the fridge. Next, they were placed in optimal cutting temperature medium (OCT) (Tissue Plus® O. C. T. Compound, Fisher HealthCare Catalog No. 4585 Lot No. 4566) in a square plastic mold, then frozen and embedded by laying the mold on top of finely crushed dry ice for several minutes after the clear colourless OCT turned opaque white. The embedded samples were wrapped in aluminum foil, placed in a sealable plastic bag, and stored at -70°C until sectioning.

It seemed that the fixative did not reach the brains as the brain sections tended to fall off the slides during immunolabelling, so the protocol was changed for the next samples. At WashU, 3-month-old wild-type (AB*) and 6-month-old *casper* zebrafish brains were isolated, fixed in 4% PFA at 4°C for approximately 20 hours, washed 3 times in 1X PBS for 10 minutes each, then stored in 1X PBS for shipping. Once the samples arrived, they were stored in the fridge. The fixed brains were then incubated overnight in the fridge with cryoprotectant, 30% sucrose in 1X PBS, followed by a second overnight incubation in the fridge in a mixture of 50% cryoprotectant and 50% OCT, then a third overnight incubation in 100% OCT in the fridge. After incubation, these samples were flash-frozen in OCT with liquid nitrogen, wrapped in parafilm and aluminum foil, placed in a sealable plastic bag, and stored at -70°C until sectioning.

While the isolated brains stuck to the slides more reliably, the sections had more cracks and damage. This may have been due to prolonged storage in the -70°C freezer or from freezing quickly in the liquid nitrogen. Additionally, the GFAP fluorescence was not as vibrant as it was in the sectioned heads, so I suspected the isolated brains were over-fixed. The approximately 2-month-old juvenile *casper* and RGC labelled Tg(*isl2b*:QF2,QUAS:loxP-mCherry-loxP-memGCaMP8m) brains were fixed in 4% PFA at 4°C for 16 hours, washed 3 times in 1X PBS for 10 minutes each, stored in 1X PBS for shipping, briefly stored in the freezer, then stored in the fridge until processing. The fixed brains were cryoprotected in 1X PBS with 30% sucrose for a couple days in the fridge, then left in OCT in the fridge for 16 days. Then, the two brains were placed in the same mold with OCT in different orientations (RGC labelled for coronal cuts, *casper* for horizontal cuts) then frozen on crushed dry ice for approximately 18 min. Immediately after freezing, the frozen block was placed in the cryostat for 1 hour to equilibrate before being sectioned the same day.

The juvenile sablefish brain was fixed in PFA for approximately 6 hours, cryoprotected in 1X PBS with 30% sucrose overnight in the fridge, transitioned to 50% 1X PBS with 30% sucrose and 50% OCT and left overnight in the fridge, then transitioned to all OCT and left overnight in the fridge. After sitting with OCT in the fridge, the brain was embedded and frozen in OCT in a 1.5 mL microcentrifuge tube placed on crushed dry ice. Immediately after freezing, the block was transferred into the cryostat, left to equilibrate, then was sectioned the same day.

10 dpf larval *casper* zebrafish were fixed for 24 hours at 4°C in 4% PFA, then washed 3 times in 1X PBS for 10 minutes each. The larvae were not cryoprotected and embedded. Instead, the larvae were labelled whole in 0.6 mL tubes. Because larval zebrafish are very small (whole body around 4 mm long (ZFIN, 2026)), cryosectioning is challenging as a few lost sections could mean losing most of the brain. Therefore, I wanted to test if I could label and image the larvae without sectioning. Labelled larvae were positioned on slides for imaging using 1.5% agarose in 1X TAE. Positioning the larvae was challenging as the gel solidified instantly, allowing no time for adjustments. A lower amount of agarose or using low-melting temperature agarose could be used to allow for more time for manipulation before the gel sets.

Due to issues with the temperature regulation mechanisms, the fridge used for storage, cryoprotection incubations, OCT incubations, and most of the antibody incubations kept samples between approximately 0-4°C.

Cryosectioning

Embedded and frozen samples were sectioned at -20°C (± 1°C) using Dr. Bob Chow's cryostat microtome (Leica CM1850UV). Sections were cut one at a time and placed on adhesive slides (NewSilane Adhesive Coated Slides, White Frosted, Newcomer Supply Cat. No. 5070), with 3-4 sections per slide. Initially, sections were 20 µm thick, which was chosen to balance imaging quality (thinner sections have less background fluorescence and allow for finer resolution of z-layers) with section quality, such as reducing folding and breakage (thicker sections). Later this was changed to 40 µm thick sections to increase section quality, paired with a longer room temperature incubation to let the antibodies penetrate deeper. The juvenile sablefish brain, juvenile *casper* brain, and juvenile RGC labelled brain were sectioned to a thickness of 40 µm, the whole mount larvae were not sectioned, and the rest of the samples were sectioned to a thickness of 20 µm. Sections were stored in the -70°C freezer until immunolabelling. The storage duration was approximately 15 hours to a couple of weeks.

Immunolabelling

Slides were taken out of the -70°C freezer and thawed for 3-5 minutes before being immersed in 1X PBS for 10 minutes to remove the OCT. Next, slides were dried with a Kimwipe and then a PAP pen (Liquid Blocker Super PAP Pen Mini, Daido Sangyo Co., Ltd. Japan, Newcomer Supply Cat. No. 6506) was used to draw a circular hydrophobic barrier around each section. 1% triton in 1X PBS was applied to each section and incubated at room temperature for either 15 minutes (for 20 µm sections) or 20 minutes (for 40 µm sections). The triton was briefly washed away by applying and quickly removing 1X PBS two to three times. The 20 µm sections were incubated for 30 minutes at room temperature with a blocking buffer (1X PBS with 2% goat serum), which then was removed, and no washes were performed before adding primary antibodies. The 40 µm sections were not incubated with blocking buffer because it did not seem to have much of an impact and I was trying to make the immunolabelling protocol more time efficient.

Primary antibodies were added to 1X PBS to dilute the antibody and create a the "primary antibody mixture", which was then applied to the sections to be labelled. "No-primary" controls received only 1X PBS with no antibodies. Samples were incubated in a dark, humid chamber, which consisted of one metal baking tray with water, paper towels, and plastic

embedding molds as slide holders, covered by one sheet of aluminum foil, then covered by another metal baking tray. The following sections were incubated overnight in the too-cold fridge: juvenile wild-type and myosin-labelled zebrafish heads, most of the isolated zebrafish brain samples, and the whole mounted larvae. The wild-type zebrafish brain sections for the lower concentration test imaged with the 60x objective lens (may later be referred to as 60x sections) and sablefish brain sections were incubated for 4 hours at room temperature; for the 60x sections this was due to lower antibody concentration, for the sablefish sections this was due to the sections being thicker. The RGC and horizontal *casper* brains were incubated overnight in a different fridge as the original fridge seemed to create "bright, large, sparkly circle" artefacts in random places on the samples that were not seen after room temperature incubations. The primary antibody mixture was removed by 2-3 brief washes with 1X PBS followed by submerging in a small container of 1X PBS for 5 minutes, then submerged in a container with fresh 1X PBS for another 5 minutes, repeated a total of three times.

Secondary antibodies were diluted with 1X PBS to create the "secondary antibody mixture". The secondary antibody mixture for samples labelled with the anti-melanopsin and anti-GFAP primary antibodies had both Alexa 555 and Alexa 488, while the mixtures for the anti-mCherry test had only one secondary antibody because only one primary antibody was applied to each section. The secondary antibody mixture was pipetted onto the sections which were then incubated for 2 hours at room temperature in the dark humid chamber. The secondary antibody mix was removed as was done for the primary mix, by pipetting on and off 1X PBS to the sections followed by 3 soaks in a small container with fresh 1X PBS for 5 minutes each.

The slides were dried and a drop of DAPI (DAPI Fluoromount-G™, Electron Microscopy Sciences Cat. No. 17984-24 Lot No. 230207, not diluted) was applied to each section. Then a cover slip (24 mm x 50 mm No. 1.5 Microscope Cover, Glass Globe Scientific Inc. Cat. No. 1415-15 Lot No. A110445-45-071023 or 22 mm x 22 mm No. 1.5 Thickness Cover Slips, Epredia, Cat. No. 152222, Lot No. 24330) was placed on top of each slide. The slides were sealed by applying clear nail polish around all edges of the cover slip and sections were left overnight in the fridge to incubate with DAPI allow the nail polish to harden.

Imaging

Sections were imaged using Dr. Bob Chow's confocal microscope (A Nikon C2) controlled by a computer running NIS-Elements (AR 4.50.00 64 bit), with the pinhole set to 30.0 μm. The objective lenses used for taking images were either the 20x air objective (numerical aperture 0.75) or the 60x oil objective (numerical aperture 1.49). The three channels used were 561 nm for Alexa 555 (OPN4L, pas350, and the anti-mCherry antibodies), 488 nm for Alexa 488 (GFAP), and 405 nm for DAPI. Images were taken with varying numbers of Z-stacks and sometimes X-Y imaging to capture a larger area of the sample.

During an imaging session, the power and gain of each channel was adjusted separately to ensure the image was as bright as possible yet minimize the number of saturated pixels (pixels where the brightness cannot become brighter by increasing power or gain) in the region of interest ("just below saturation"). This increases the image resolution and contrast, the range of shades of pixels in the image, which can be important for downstream analyses (Visscher *et al*., 1994; Brown, 2007; discussed in BIOL 5508, Advanced Methods in Vision Science at WashU in Spring 2025). For the 488 nm and 561 nm channels, the power and gain were lowered slightly further below saturation to reduce some of the overall background brightness for visual clarity as these images were being qualitatively examined by eye. For samples imaged with the 60x objective lens, the pixel dwell was lowered, the power was raised, the LUT channels were adjusted to increase the brightness by eye, and a subset of the imaging field was used to try to obtain higher resolution images. Controls were imaged with power and gain settings matching or very close to those used for at least one other sample on the same slide. Different samples on the same slide were often but not always imaged with the same power and gain settings during an imaging session.

The z-steps were adjusted to capture the whole thickness of the sample which was determined using the DAPI (nuclear) staining. Samples tended to have nuclei that were clear in one plane yet absent from or faint in another, usually with the superficial white and grey zone being most visible in a different plane than the periventricular grey zone. This approach led to an inconsistent number of and distances between z-layers. The number of z-steps was sometimes reduced to minimize imaging time, for example one full zebrafish brain with 3 z-layers and 3 channels took approximately an hour to image.

Once the images were acquired, the microscope's imaging software (NIS-Elements AR 4.50.00 64 bit) was used to stitch together large images (*i.e.*, those with X-Y imaging) and flatten z-layers into 2D maximum intensity projections.

Data Analysis

Brain regions of adult zebrafish were identified by comparison with the adult zebrafish brain atlas (AZBA) (Kenny *et al*., 2021), a book on zebrafish neuroanatomy (Wullimann *et al*., 1996), Mueller (2012)'s publication, and Jurisch-Yaksi *et al*. (2020)'s study. Brain regions of larval zebrafish were identified by comparison with the Zebrafish UCL website (https://zebrafishucl.org/zebrafishbrain#explore-the-brain), Jurisch-Yaksi *et al*. (2020)'s study, and the Z Brain Atlas (Randlett *et al*., 2015).

Image analysis was done qualitatively. Controls (no primary antibody added but otherwise treated the same) were compared to labelled sections of similar brain regions, which were consecutive sections or one of the closest non-consecutive sections. Areas that were brighter in the labelled sections were deemed potential areas of interest (for OPN4L or pas350) or labelling (for GFAP and DAPI). Areas of interest that consistently appeared across different individuals were interpreted as labelling by the primary antibody and thereby considered to indicate presence of the protein the antibody was designed to bind.

After analysis, images were given scale bars in FIJI (Fiji Is Just ImageJ version 1.54p, Java 1.8.0_322 (64-bit)), small insets of the images were cropped using ImageJ's BioVoxxel add-on (BioVoxxel: Figures Tools version 4.1.0 https://doi.org/10.5281/zenodo.14217141), the images and insets were combined into figures in Microsoft PowerPoint and the brightness of some images were increased in PowerPoint to even out visibility across images. Both brightness and contrast for all confocal figures (*i.e.*, all the panels get the same adjustment) was increased by 20% in Microsoft Word to increase visibility of all the images.

Results

Antigen Sequence Specificity

The sequence of the synthetic peptide conjugated to KLH that the OPN4L antibody was raised against appeared to be "TIRAAGKEIRELDCGETHKVYERMQNEWKMAKVA". The

alignment of the zebrafish melanopsins on NCBI clarified the multiple alternative names for the melanopsin genes (Table 3, Figure 1).

Table 3. Zebrafish melanopsin gene names, chromosome locations, and alternative names.

Gene	Chromosome	Alternative Names (NCBI, 2025; ZFIN, 2025)
opn4m1	13	*opn4*, *opn4a*, *opn4d*
opn4m2	2	*opn4*, *opn4.1*, *opn4l*, *opn4c*
opn4m3	12	*opn4b*, *opn4l2*
opn4x1	10	*opn4x-1*, *opn4xa*
opn4x2	5	*opn4x-2*, *opn4xb*, *opn4x1*, si:dkeyp-100d11.3

Using NCBI to BLAST search for the OPN4L immunogen sequence against zebrafish and sablefish resulted in finding melanopsins, mainly *opn4m2*, some melanopsin-like proteins, or matches to regions of chromosome 2 (the most similar proteins would be other melanopsins, and the only melanopsin known to be present on that chromosome is *opn4m2*) (Appendix A). There were some matches to other melanopsins, such as *opn4a* (*opn4m1*) in zebrafish and melanopsin-A (*opn4m1*) in sablefish. OPN4L's immunogen sequence matches the best to zebrafish *opn4m2* (Figure 1). Of the sablefish melanopsins, *opn4m2* shows the best match with the OPN4L immunogen sequence, however it is still quite different.

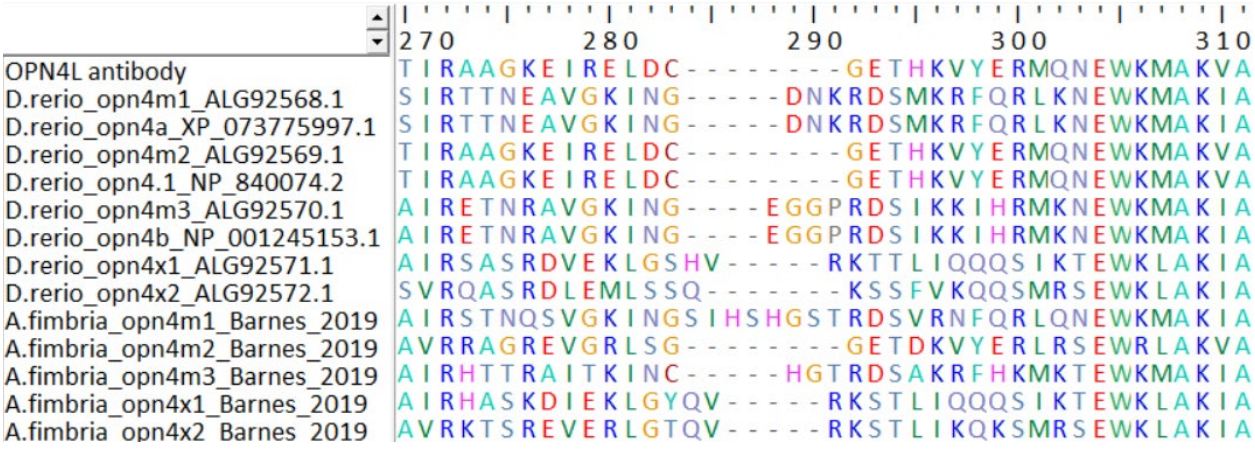

Figure 1. Amino acid alignment of the OPN4L antigen sequence, zebrafish (*Danio rerio*) melanopsins, and sablefish (*Anoplopoma fimbria*) melanopsins. Sequences were collected from NCBI or Barnes (2022). The multiple sequence alignment was created with ClustalW v. 1.4, accessory application in BioEdit v. 7.7.1. The antigen sequence was manually aligned.

The melanopsin part of the conjugate peptide that pas350 (Davies *et al*., 2011) was raised against is a good match for the three zebrafish *opn4m*s, and roughly a half-match for the two zebrafish *opn4x*s (Figure 2). However, it is not a perfect match to the zebrafish *opn4m*s with the first two amino acids mismatching (CV compared to VY, PH, or RH). As Barnes (2022) found, pas350 is similar to the three sablefish *opn4m*s, however sablefish *opn4m2* has one less matching amino acid than the other two. The similarity in sequence between zebrafish and sablefish shows that pas350 binds a conserved domain in teleost melanopsins.

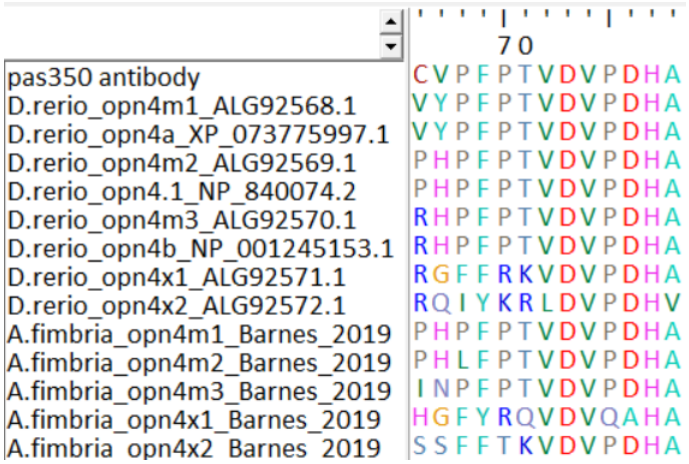

Figure 2. Amino acid alignment of the pas350 antigen sequence, zebrafish (*Danio rerio*) melanopsins, and sablefish (*Anoplopoma fimbria*) melanopsins. The sequences were collected from NCBI or Barnes (2022). The multiple sequence alignment was created with ClustalW v. 1.4, accessory application in BioEdit v. 7.7.1. The antigen sequence was manually aligned.

The only match to keyhole limpet hemocyanin sequences was KLH1 to a chromosome 25 in zebrafish (Appendix A). This match is not in a coding region and the closest gene is TAFA chemokine like family member 5b (tafa5b, GeneID: 100536289) which is approximately 54,000 nucleotides away.

Section and Labelling Quality

In most of the sections, DAPI (nuclear stain) labelling looks as expected from other publications (Corbo *et al*., 2012; Lindsey *et al*., 2019; Kenny *et al*., 2021), which indicates good section histology. Sometimes the DAPI staining was dim, suggesting that the maximum intensity projection image was not capturing that region, either due to needing to include more z-layers or

due to tissue damage. GFAP (antibody against a glial marker) labelling was used to assess the immunolabelling quality. GFAP labelling was reliably present where expected (Than-Trong and Bally-Cuif, 2015), indicating immunolabelling was working. However, GFAP labelling was faint in the brain sections, suggesting that the methodology could use some improvements to increase the quality of antibody labelling.

Protocol variations impacted the quality of sections. Steps that led to better cryosectioning (fewer cracks in the tissue breaking, fewer lost sections) included freezing with dry ice (rather than liquid nitrogen), immediately being transferred to the -20°C cryostat to equilibrate for at least 1 hour (rather than being stored in the -70°C freezer, equilibrated for 10 minutes, then sectioned), and sectioning to 40 µm thick (rather than 20 µm). Examples of better sections are Figure 3 panels E and F, and examples of more damaged sections are Figure 3 panels G and H. I acquired 52 consecutive 40 µm sections of the RGC labelled brain, starting from early telencephalon and ending somewhere in the medulla. Using that information, I estimated that a 2-month-old zebrafish brain is at least approximately 2080 µm (or 2.08 mm) long from anterior to posterior in lieu of measuring it with a ruler or scalebar. However, upon a closer look with the confocal microscope, it appears something happened to the histology of the RGC labelled brain making it too difficult to discern much labelling. It was not just the RGC labelled brain, the horizontal sections of the juvenile *casper* brain that was processed at the same time had the same strange histology (data not shown).

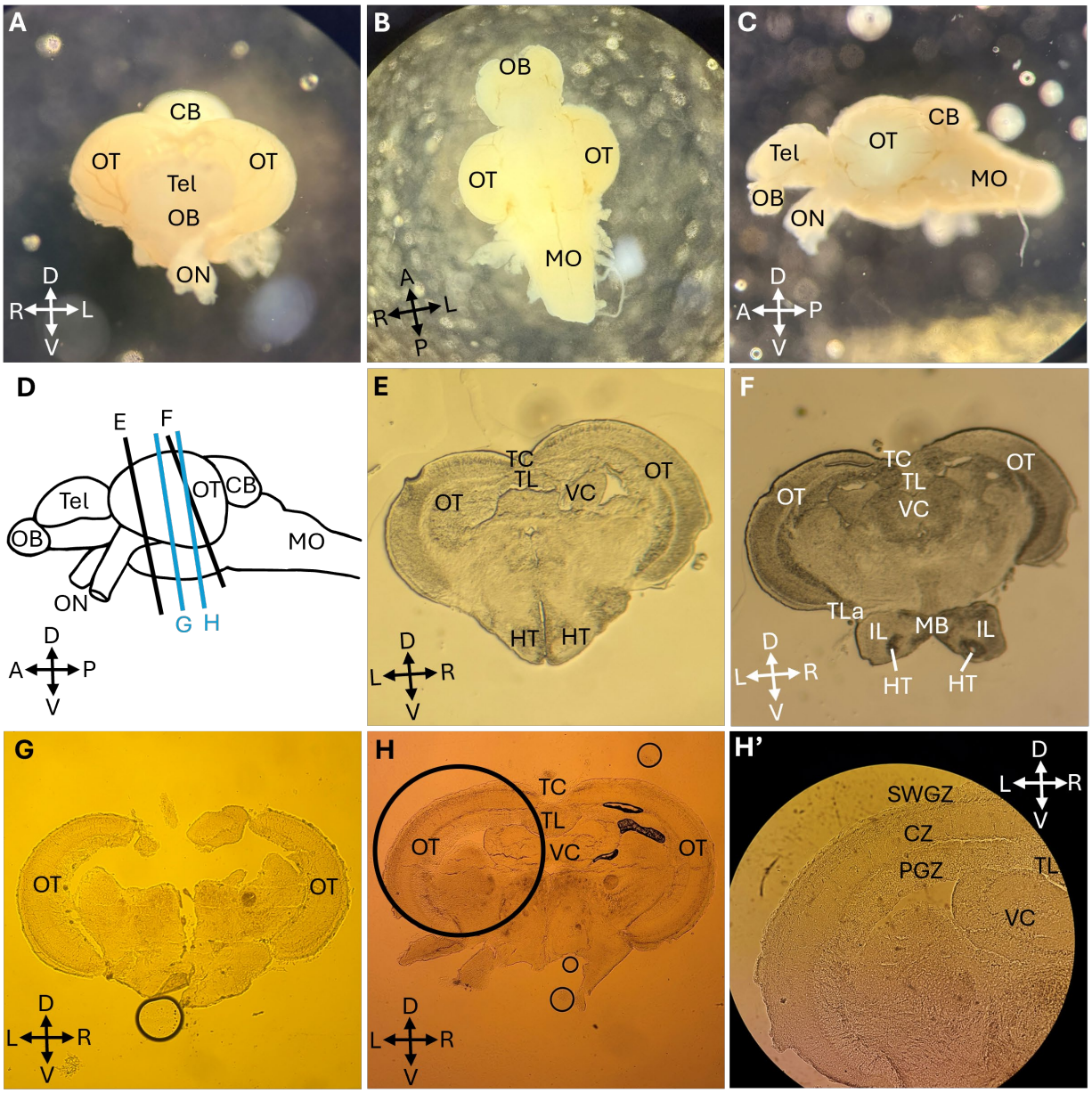

Figure 3. Photos of whole and sectioned adult zebrafish (*Danio rerio*) brains. (A) Coronal view of a whole brain in OCT with the anterior portion facing the camera. (B) Ventral view of a whole brain in OCT. (C) Sagittal view of a whole brain in OCT with the left side facing the camera. (D) Diagram of the sagittal view of a whole zebrafish brain with lines indicating approximate locations of sections in panels (E-H'). (E-F) Freshly cut 20 µm thick coronal sections from one zebrafish's brain (note: the right side is more posterior than the left side). (G-H') Immunolabelled 20 µm thick coronal sections of a different zebrafish's brain. The large black circle in (H) indicates the region shown in panel at a higher (continued on the next page)

magnification in panel (H'). All photos were taken with a phone camera held to see through one eyepiece of a dissecting scope (panels A, B, and C), a different dissecting scope (panels E and F), or the confocal microscope using its brightfield mode (panels G, H, and H'). Panel H' had its brightness and contrast both increased by 20% using PowerPoint. This figure lacks scale bars as the magnifications were not recorded when the photos were taken. Abbreviations: A = anterior, CB = cerebellum, CZ = central zone of the optic tectum, D = dorsal, HT = hypothalamus, IL = inferior lobe, L = left side of fish, MB = mamillary body, MO = medulla oblongata, OB = olfactory bulb, ON = optic nerve, OT = optic tectum, P = posterior, PGZ = periventricular grey zone of the optic tectum, R = right side of fish, SWGZ = superficial white and grey zone of the optic tectum, TC = tectal commissure, Tel = telencephalon, TL = torus longitudinalis, TLa = torus lateralis, V = ventral, VC = valvula cerebelli.

OPN4L Brain Labelling

Adult wild-type zebrafish showed OPN4L labelling in two areas of the optic tectum (Figure 4). There was diffuse labelling in the superficial white and grey zone (SWGZ) and a distinct layer within the central zone (CZ) (Figure 4 panels E and E'). There was also labelling in two large cells on the right side of the paraventricular organ (PVO) (Figure 4 panels G and G'). Given the hints of fluorescence on the left side and that sections are slightly skewed, there are likely four large cells, two on each side. The optic tectum labelling was present across various antibody dilutions and in two different individuals (Figure 5). The SWGZ labelling differed between the two wild type fish where one fish had labelling in the whole SWGZ while the other only showed labelling in the ventral (deeper) half of the SWGZ (Figure 5). With the 20x objective lens, the antibody dilution where the optic tectum labelling was most distinct was OPN4L 1:500 Alexa 555 1:1000 (Figure 2), however at higher magnifications this proved to be an unnecessarily high concentration as labelling was also visible in sections labelled with a 1:10,000 dilution (Figure 6, panels E and E'). With the 60x objective lens (Figure 6), the melanopsin labelling in the CZ did not overlap with GFAP or DAPI. In the section with OPN4L diluted 1:10,000, labelling was only detectable in the maximum intensity projection, and not individual z-layers. There were also numerous very small bright dots that remained even at the lowest dilution and were present throughout the brain (Figure 6, panels F, F'). Following

individual dots across Z-layers shows that a dot persisted over a few layers but were not present in the same spot throughout the entire stack of Z-layers.

Labelling with OPN4L was similar in two *casper* zebrafish brains (Figure 7), with both showing the line of labelling in the CZ. However, the CZ line was fainter and did not cover the entirety of the optic tectum, with labelling stronger medially and fading laterally. One of the *casper* fish had diffuse labelling only in the deeper layers of the SWGZ (Figure 7 panels D and D') similar to one of the wild types (Figure 5 panel K), while the other showed no labelling in the SWGZ.

The RGC labelled (Tg(*isl2b*:QF2,QUAS:loxP-mCherry-loxP-memGCaMP8m)) zebrafish brain was of poor quality, making it difficult to discern the labelling. When looking with wide field and confocal microscopy before immunolabelling, there did not appear to be any remaining mCherry fluorescence. After labelling, under wide field microscopy none of the antibodies showed any labelling (rat anti-RFP, rabbit anti-dsRed, OPN4L) (data not shown). However, the two sections that were checked under the confocal microscope (OPN4L, rabbit anti-dsRed) showed brighter fluorescence in the SWGZ with OPN4L and in the SWGZ and entire CZ with rabbit anti-dsRed (Figure 8).

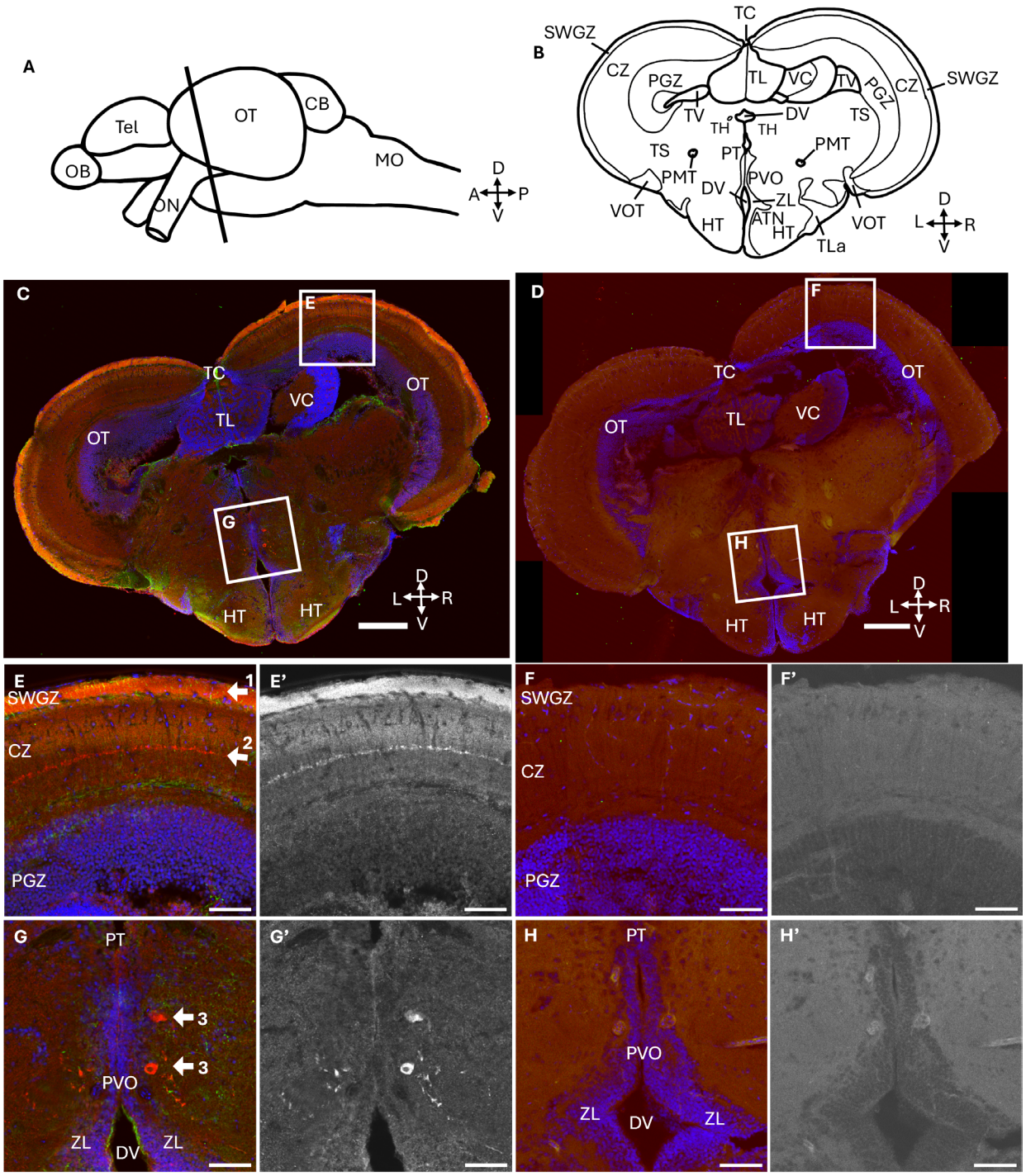

Figure 4. OPN4L labelling in a 3-month-old (adult) wild-type zebrafish (*Danio rerio*) brain sectioned into 20 µm thick coronal pieces. (A) Diagram of a whole zebrafish brain from a sagittal view with a line showing the approximate location of the sections in this figure. (B) Diagram of a coronal section of the zebrafish brain. (C, D) Coronal sections labelled with a nuclear stain (DAPI, blue), and either two primary antibodies (continued on the next page)

OPN4L (anti-*opn4m2*, diluted 1:500, red) and a glial cell marker (anti-*GFAP*, diluted 1:1600, green) (C) or no primary antibodies (D), with the location of insets E-H marked by white squares. Secondary antibodies used were Alexa 555 diluted 1:1000 and Alexa 488 diluted 1:500. (E, E') Labelled optic tectum. (F, F') No primary control optic tectum. (G, G') Labelled paraventricular organ. (H, H') No primary control of paraventricular organ. White arrows point towards labelling in (1) the superficial white and grey zone of the optic tectum, (2) the central zone of the optic tectum, and (3) large cells in the paraventricular organ. Colour images are three channels merged (405 nm, 488 nm, 561 nm) and greyscale images are only the 561 nm channel (red). The brightness was increased in ImageJ for the 488 nm (green) and 561 nm (red) channels for the no-primary control panels (D, F, F', H, H'). Abbreviations: A = anterior, ATN = anterior tuberal nucleus, CB = cerebellum, CZ = central zone, D = dorsal, DV = diencephalic ventricle, HT = hypothalamus, L = left, OB = olfactory bulb, ON = optic nerve, OT = optic tectum, P = posterior, PGZ = periventricular grey zone, PMT = pretecto-mammillary tract, PT = posterior tuberculum, PVO = paraventricular organ, Tel = telencephalon, TH = thalamus, MO = medulla oblongata, R = right, SWGZ = superficial white and grey zone, TC = tectal commissure, TL = torus longitudinalis, TLa = torus lateralis, TV = tectal ventricle, V = ventral, VC = valvula cerebelli, VOT = ventrolateral optic tract, ZL = zona limitans. Scale bars for C and D are 200 µm, and for E-H are 50 µm.

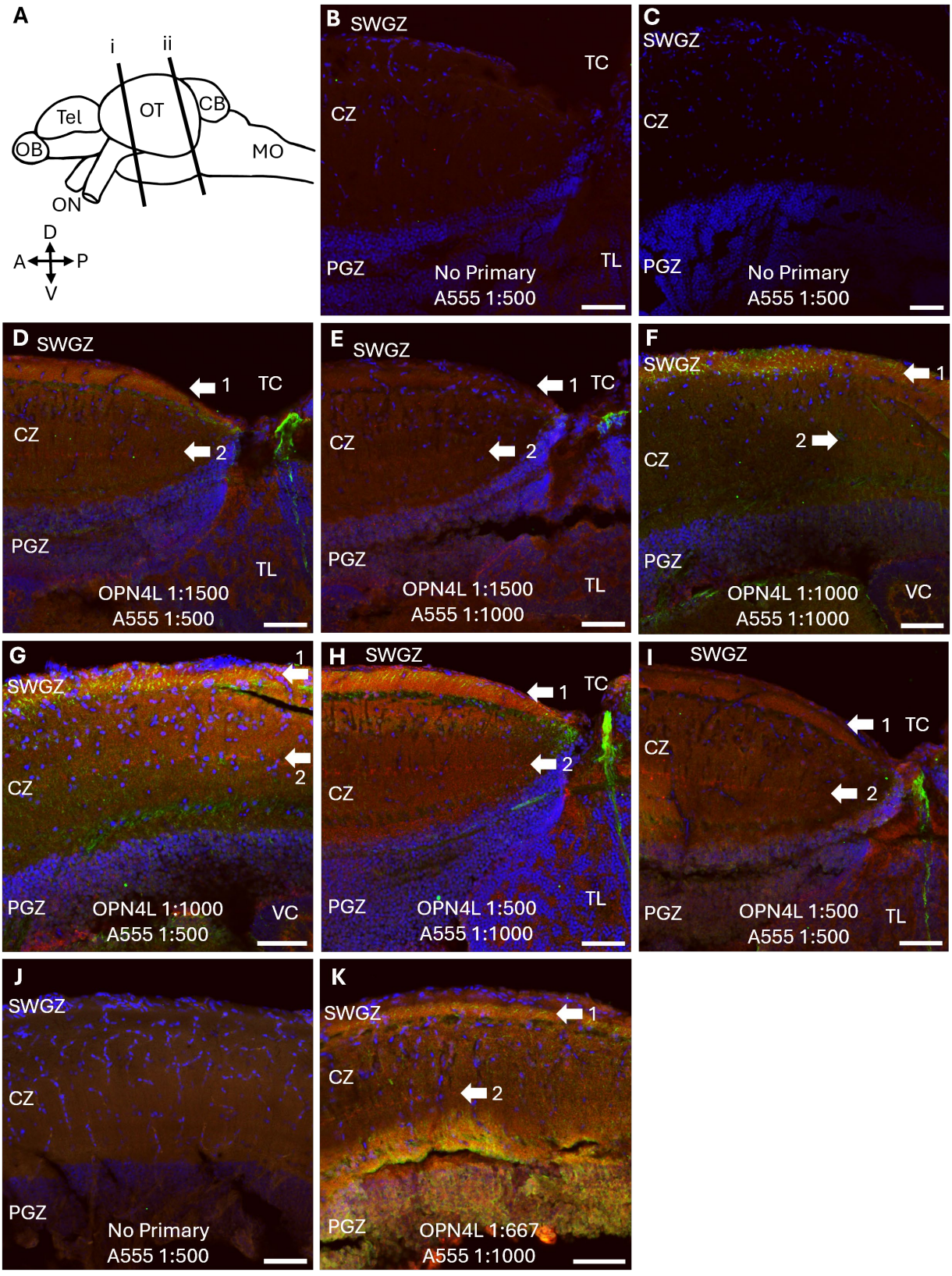

(Figure caption on the next page.)

Figure 5. OPN4L and Alexa 555 dilution test in zebrafish (*Danio rerio*) optic tectum. Two adult wild-type zebrafish brains coronally sectioned to 20 µm thick and labelled with four dilutions of OPN4L (red, anti-*opn4m2*) paired with two dilutions of Alexa 555, two dilutions of GFAP (green, glial cell marker, marked by Alexa 488 diluted 1:500), and DAPI (blue, nuclear stain). (A-I) Sections from one fish, and (J-K) sections from a different individual. (A) Diagram showing relative locations of sections where line i is the approximate location for panels B, D, E, H, I, J, and K, and line ii is the approximate location for panels C, F, and G. (B) No primary control of relatively anterior optic tectum section, Alexa 555 diluted 1:500. (C) No primary control of a relatively posterior optic tectum section, Alexa 555 diluted 1:500. (D) OPN4L diluted 1:500, Alexa 555 diluted 1:1000, GFAP diluted 1:1600. (E) OPN4L diluted 1:1500, Alexa 555 diluted 1:500, GFAP diluted 1:1600. (F) OPN4L 1:1000, Alexa 555 1:1000, GFAP 1:1600. (G) OPN4L 1:1000, Alexa 555 1:500, GFAP 1:1600. (H) OPN4L 1:500, Alexa 555 1:1000, GFAP 1:1600. (I) OPN4L 1:500, Alexa 555 1:500, GFAP 1:1600. (J) No primary control, Alexa 555 1:500. (K) OPN4L 1:667, GFAP 1:1333, Alexa 555 1:500. White arrows point toward OPN4L labelling in the (1) superficial white and grey zone and (2) central zone. Abbreviations: A = anterior, A555 = Alexa 555 secondary antibody, CZ = central zone of the optic tectum, D = dorsal, P = posterior, PGZ = periventricular grey zone of the optic tectum, SWGZ = superficial white and grey zone of the optic tectum, TC = tectal commissure, TL = torus longitudinalis, V = ventral, VC = valvula cerebelli. Scale bars = 50 µm.

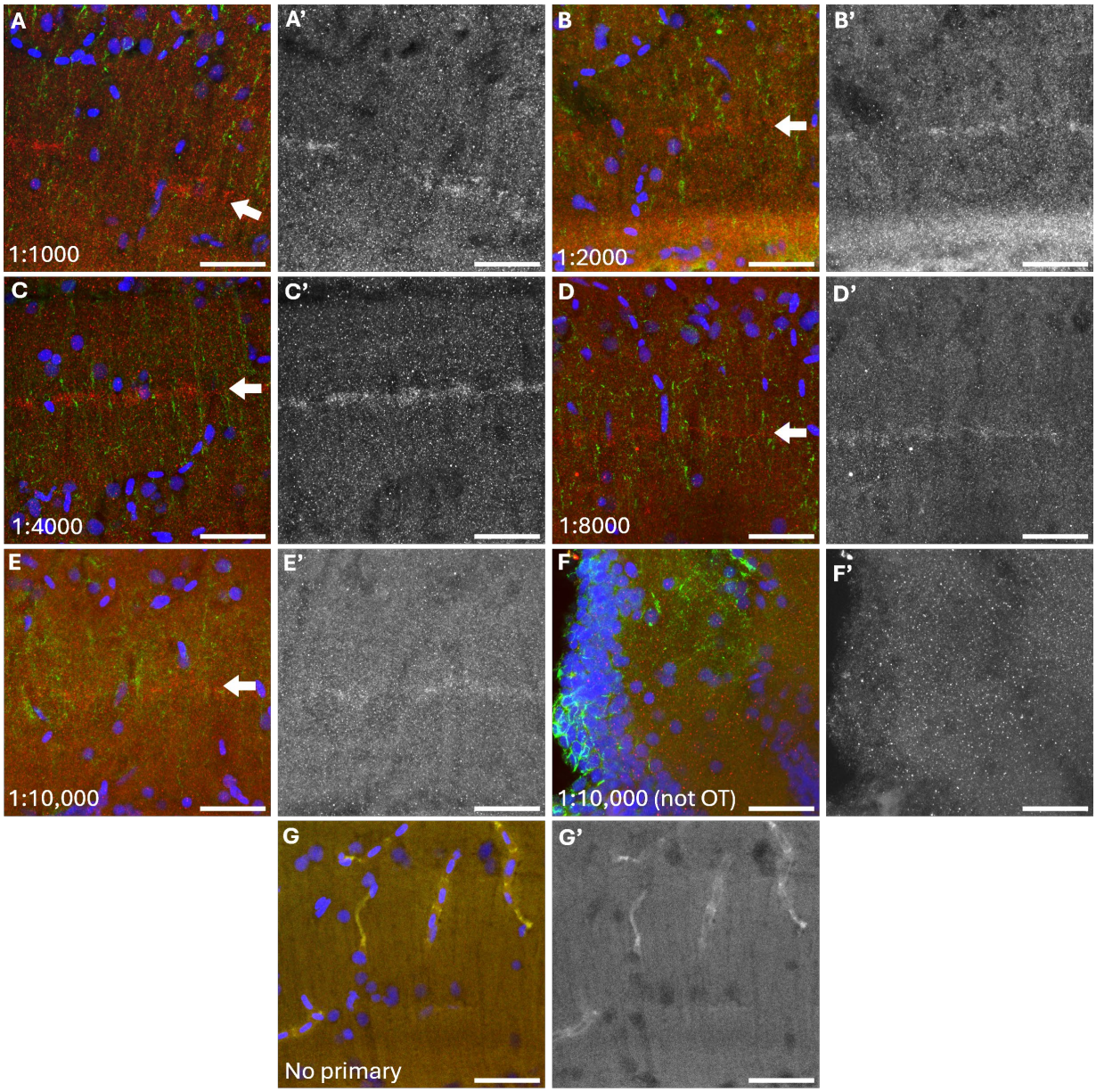

Figure 6. OPN4L labelling in the central zone of the optic tectum of two adult wild-type zebrafish (*Danio rerio*) observed with the 60x objective lens. The coronal sections were sliced to a thickness of 20 µm, then immunolabelled with five dilutions of OPN4L (anti-*opn4m2*, red), a glial cell antibody (anti-*GFAP*, green) diluted :1600, Alexa 555 diluted 1:1000, Alexa 488 diluted 1:1600, and stained with a nuclear stain (DAPI, blue). Two individuals were imaged, where panels A, B, and G are one individual, and panels C, D, E, and F are another individual. (A, A') OPN4L 1:1000, (B, B') OPN4L 1:2000, (C, C') OPN4L 1:4000, (D, D') OPN4L 1:8000, (E, E', F, F') OPN4L 1:10000), (G, G') no primary control. (continued on the next page)

White arrows point to examples of melanopsin labelling. Brightness has been adjusted in ImageJ (staring with “auto” adjust in all three channels followed by reducing the brightness of the 488 nm channel and sometimes slightly reducing brightness of the 561 nm channel) for all channels in all the panels of this figure as they were imaged with LUT’s adjusted and would otherwise appear too dark. Colour images show the three channels merged (405 nm in blue, 488 nm in green, 561 nm in red), and greyscale images are just of the 561 nm channel (red). Abbreviation: OT = optic tectum. Scale bars = 25 µm.

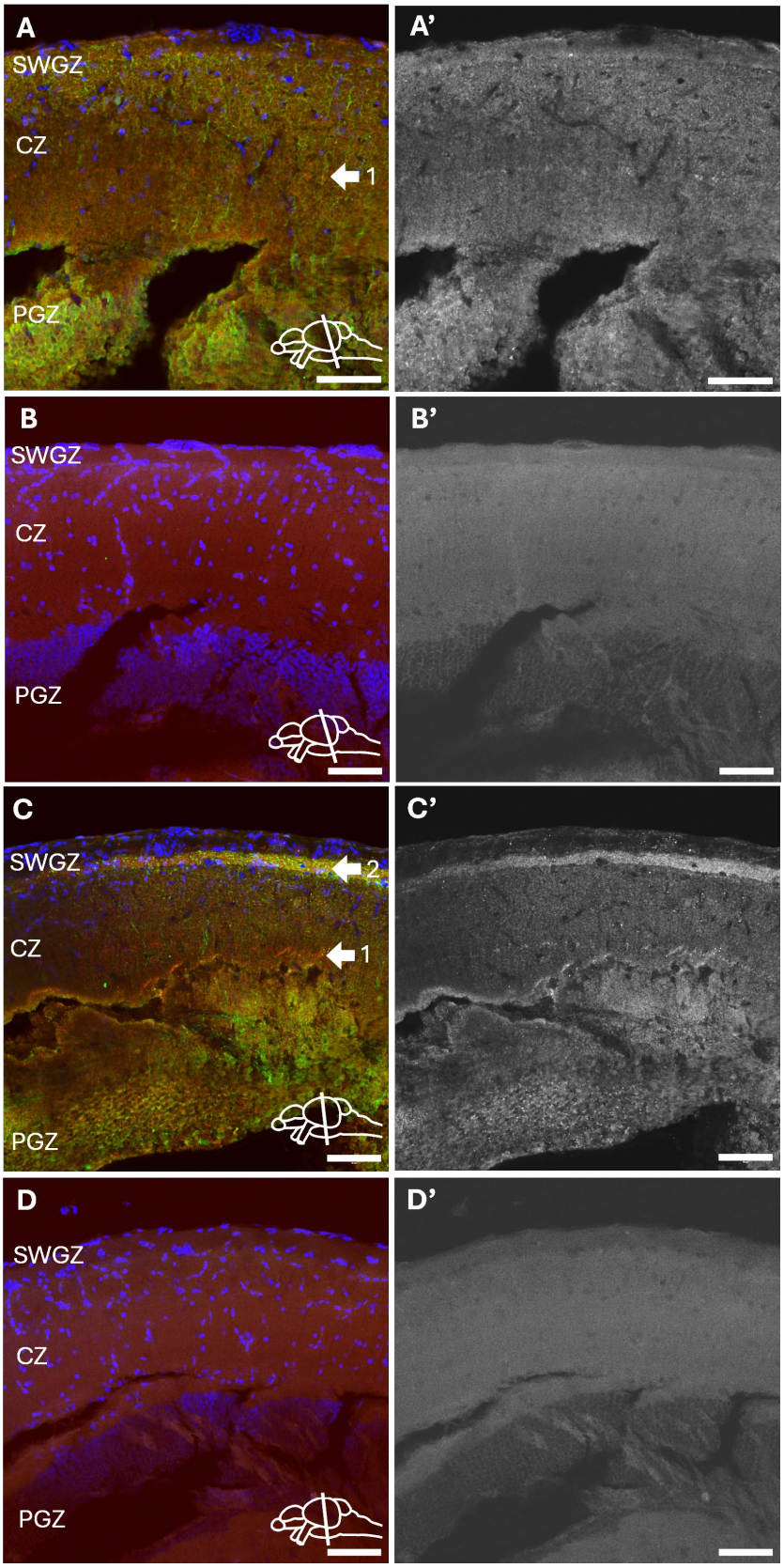

(Figure caption on the next page.)

Figure 7. OPN4L labelling of two 6-month-old (adult) *casper* zebrafish (*Danio rerio*) optic tecta. The coronal sections were 20 µm thick and labelled with two primary antibodies (A, C) OPN4L (anti-*opn4m2*, red) diluted 1:667, or no primary antibodies (B, D), a glial marker (anti-*GFAP*, green) diluted 1:1333, and a nuclear stain (DAPI, blue). The secondary antibodies used were Alexa 555 diluted 1:1000, and Alexa 488 diluted 1:500. (A, B) are one individual, (C, D) are another individual. White arrows point towards OPN4L labelling in (1) the central zone and (2) superficial white and grey zone. The white lines in the small diagrams of brains from a sagittal view indicate the approximate location of the section. Colour images (A, B, C, D) are the three channels merged showing all the labelling, while greyscale images (A', B', C', D') show only the 561 nm channel (red). Abbreviations: CZ = central zone of the optic tectum, PGZ = periventricular grey zone of the optic tectum, SWGZ = superficial white and grey zone of the optic tectum. Scale bars = 50 um.

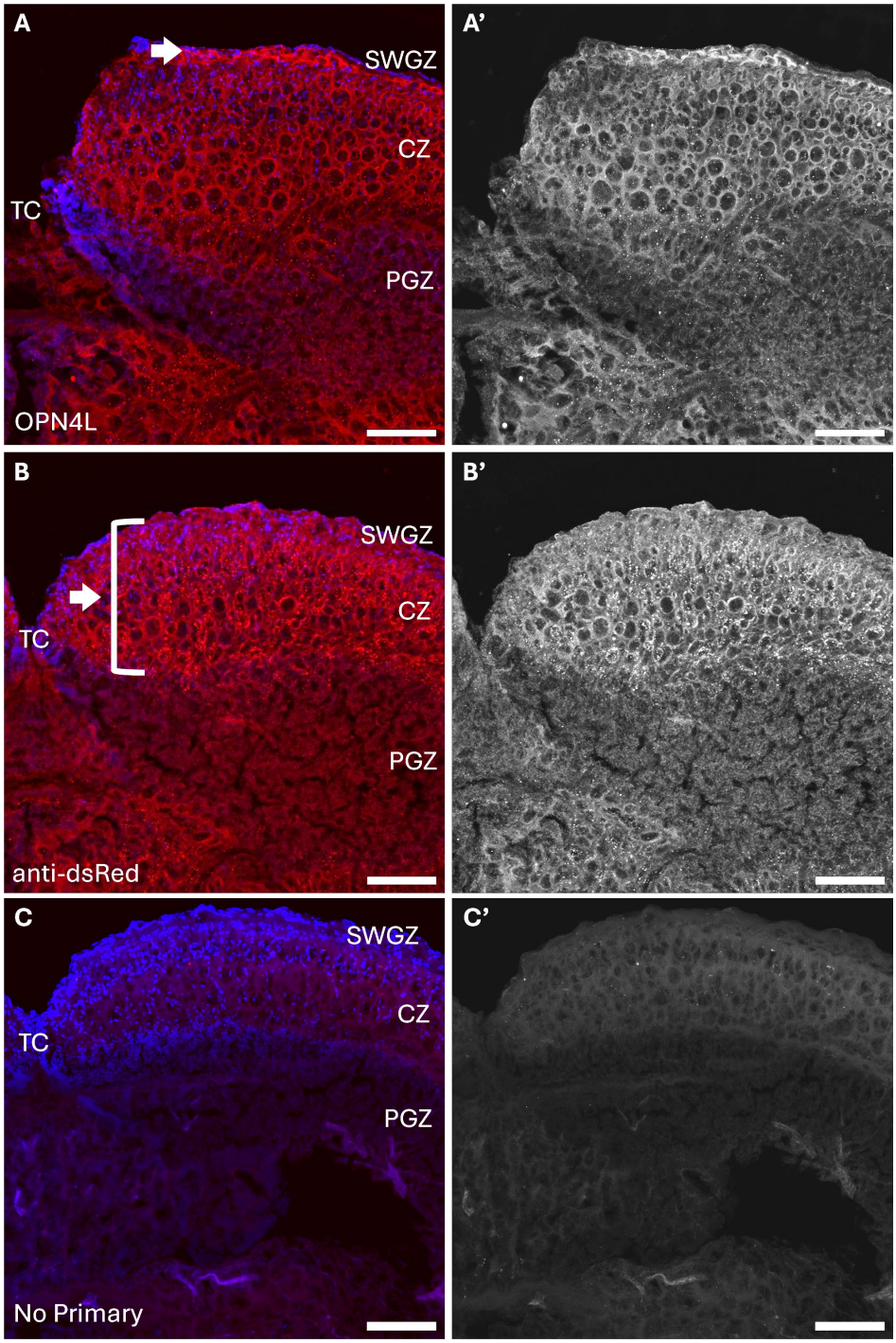

Figure 8. 40 µm thick coronal sections of the optic tectum of a 2-month-old (juvenile) retinal ganglion cell labelled (Tg(*isl2b*:QF2,QUAS:loxP-mCherry-loxP-memGCaMP8m)) zebrafish (*Danio rerio*). (A, A') Labelled with OPN4L diluted 1:2000 with the usual secondary antibody. (B, B') Labelled with rabbit anti-dsRed diluted 1:250 with the same secondary as C. (C, C') No primary control labelled with Alexa 555 (red) diluted 1:500 and (continued on the next page)

a nuclear stain (DAPI, blue). Colour images (A, B, C) show the two imaging channels merged (405 nm, 561 nm), and greyscale images (A', B', C') show only the 561 nm channel (red). White arrows point towards the potential labelling. Note: there were issues with the histology making it difficult to see much beyond general patterns. Due to this, panel C's 405 nm channel (DAPI) was made brighter (higher power and gain) to capture nuclei in the periventricular grey zone, however it made the superficial white and grey zone nuclei appear far more prominent than normal. Abbreviations: CZ = central zone, PGZ = periventricular grey zone, SWGZ = superficial white and grey zone, TC = tectal commissure. Scale bars = 100 μm.

pas350 Brain Labelling

At the dorsal side of the zebrafish brain, pas350 labelled faint dots across the optic tectum, mostly in the more superficial layers of the CZ, processes in the torus longitudinalis (TL), and cells in the periventricular grey zone (Figure 9). At the ventral side of the zebrafish brain, pas350 labelled dots in the torus lateralis (TLa), inferior lobe (IL), and hypothamus (HT) (Figure 10). Many of the dots of labelling overlapped with DAPI. TL labelling overlapped with GFAP labelling (Figure 9 panels C-C''). This pattern of pas350 labelling was present across two dilutions of pas350 and two dilutions of Alexa 555 (total 4 antibody mixtures), although the visibility of the labelling varied (data not shown).

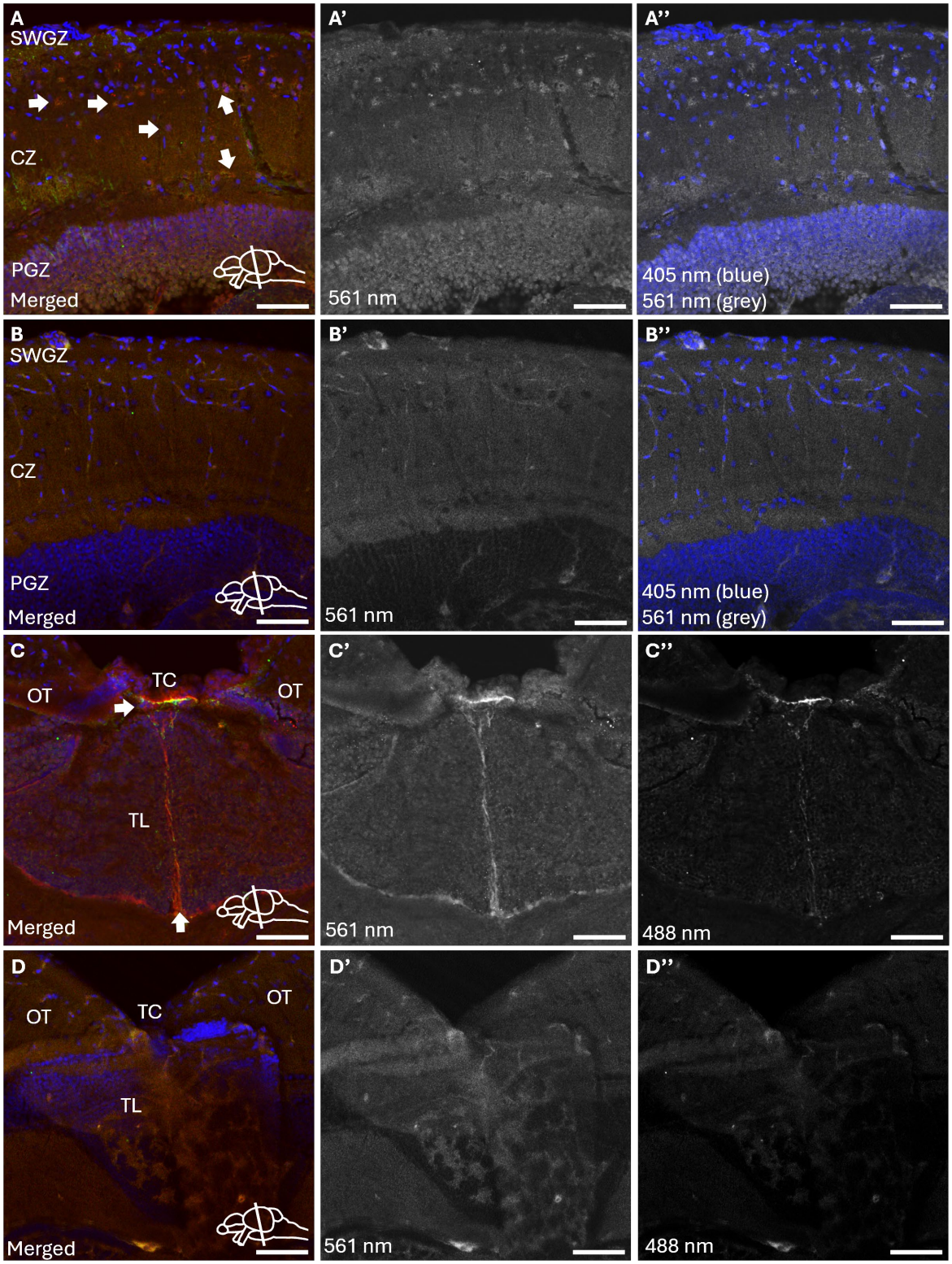

Figure 9. Dorsal regions of coronal sections of a wild-type zebrafish (*Danio rerio*) brain sectioned to 20 µm thick and labelled with (continued on the next page)

pas350 (anti-*opn4m1*, *opn4m2*, and *opn4m3*, red; with Alexa 555), a glial marker (anti-*GFAP*, green, diluted 1:1600; with Alexa 488 diluted 1:500), and a nuclear stain (DAPI, blue). (A) Optic tectum labelled with pas350 diluted 1:250 and Alexa 555 diluted 1:1000. (B) No primary control of optic tectum with Alexa 555 diluted 1:1000. (C) Torus longitudinalis with pas350 diluted 1:500 and Alexa 555 diluted 1:500. (D) No primary control of torus longitudinalis with Alexa 555 diluted 1:1000. Colour images (A, B, C) show all three channels merged, greyscale images show only either the 561 nm channel (red, panels A', A'', B', B'', C', and D') or 488 nm channel (green, GFAP, panels C'' and D''), and greyscale with blue show the 561 nm channel in grey with 405 nm channel (DAPI) in blue (panels A'', B''). White arrows point towards examples of pas350 labelling. Small white diagrams of a sagittal view of a whole brain indicate the approximate location of the section with a white line. Abbreviations: CZ = central zone of the optic tectum, OT = optic tectum, PGZ = periventricular grey zone of the optic tectum, SWGZ = superficial white and grey zone of the optic tectum, TC = tectal commissure, TL = torus longitudinalis. Scale bars = 50 μm.

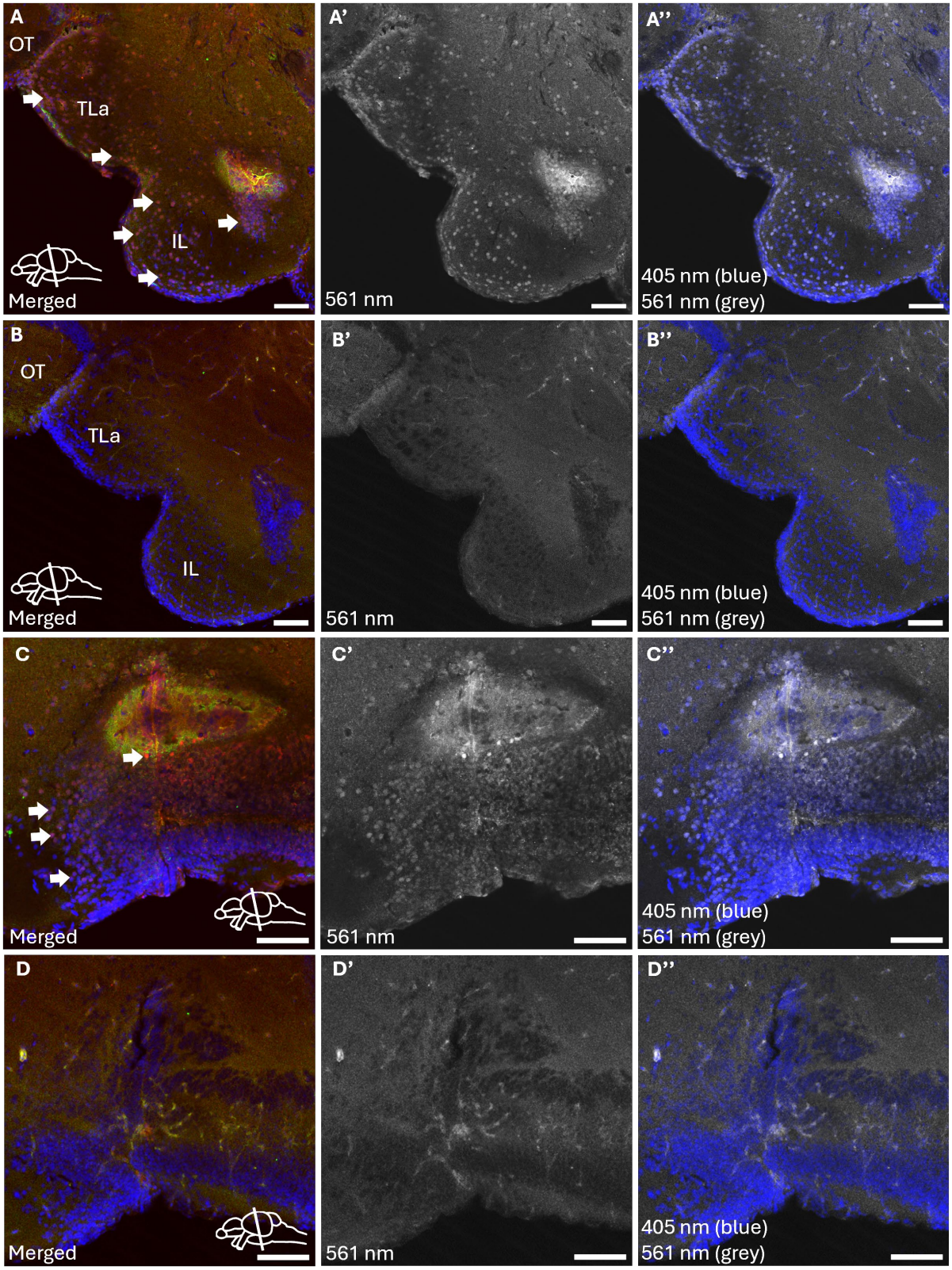

Figure 10. Ventral regions of coronal sections of an adult wild-type zebrafish (*Danio rerio*) brain sectioned to 20 µm thick and labelled with (continued on the next page)

pas350 (red, anti-*opn4m1*, *opn4m2*, and *opn4m3*, diluted 1:250; with Alexa 555 diluted 1:1000), a glial marker (green, anti-*GFAP*, diluted 1:1600; with Alexa 488 diluted 1:1000), and a nuclear stain (blue, DAPI). (A) Labelled area to the left of the hypothalamus. (B) No primary control of area to the left of the hypothalamus. (C) Labelled hypothalamus. (D) No primary control of the hypothalamus. White arrows point towards examples of pas350 labelling. The very bright patches in multiple channels in A and C might be labelling artefacts or not catching the appropriate z-layers to capture those patches accurately. Abbreviations: IL = inferior lobe, OT = optic tectum, TLa = torus lateralis. Scale bars = 50 μm.

Sablefish Sections

In the juvenile sablefish brain, OPN4L labelled the walls of blood vessels and a few spots across the optic tectum that tended to be on top of blood vessels and, upon inspection by scrolling through Z-layers, often appeared to be in indents in the tissue (Figure 11).

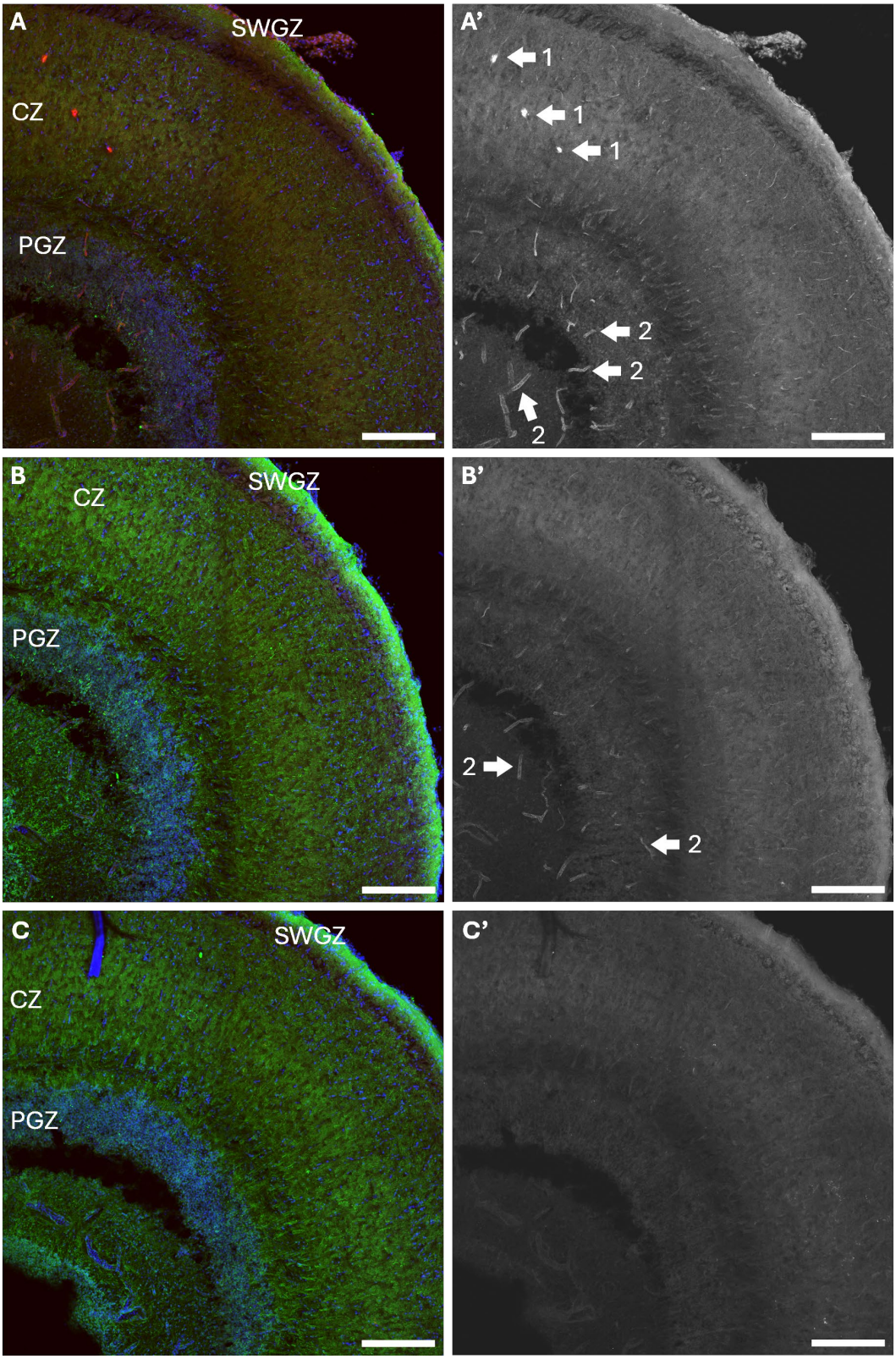

Figure 11. Juvenile sablefish (*Anoplopoma fimbria*) optic tectum sectioned into 40 µm thick coronal slices labelled with (continued on the next page)

OPN4L (red, anti-*opn4m2*; with Alexa 555 diluted 1:1000), a glial marker (green, anti-*GFAP* diluted 1:1600; with Alexa 488 diluted 1:500), and a nuclear stain (blue, DAPI). (A) OPN4L diluted 1:1000. (B) OPN4L diluted 1:4000. (C) No OPN4L control with GFAP. White arrows point towards examples of melanopsin labelling in (1) spots in the central zone and (2) blood vessels. Abbreviations: CZ = central zone of the optic tectum, PGZ = periventricular grey zone of the optic tectum, SWGZ = superficial white and grey zone of the optic tectum. Scale bars = 200 μm.

Zebrafish Retinas

In the zebrafish retina, pas350 labelled projections in the ganglion cell layer, likely retinal ganglion cells as the projections were diagonal to the GFAP which labels Muller glia, and cell bodies in the inner nuclear layer, likely amacrine cells (Figure 12).

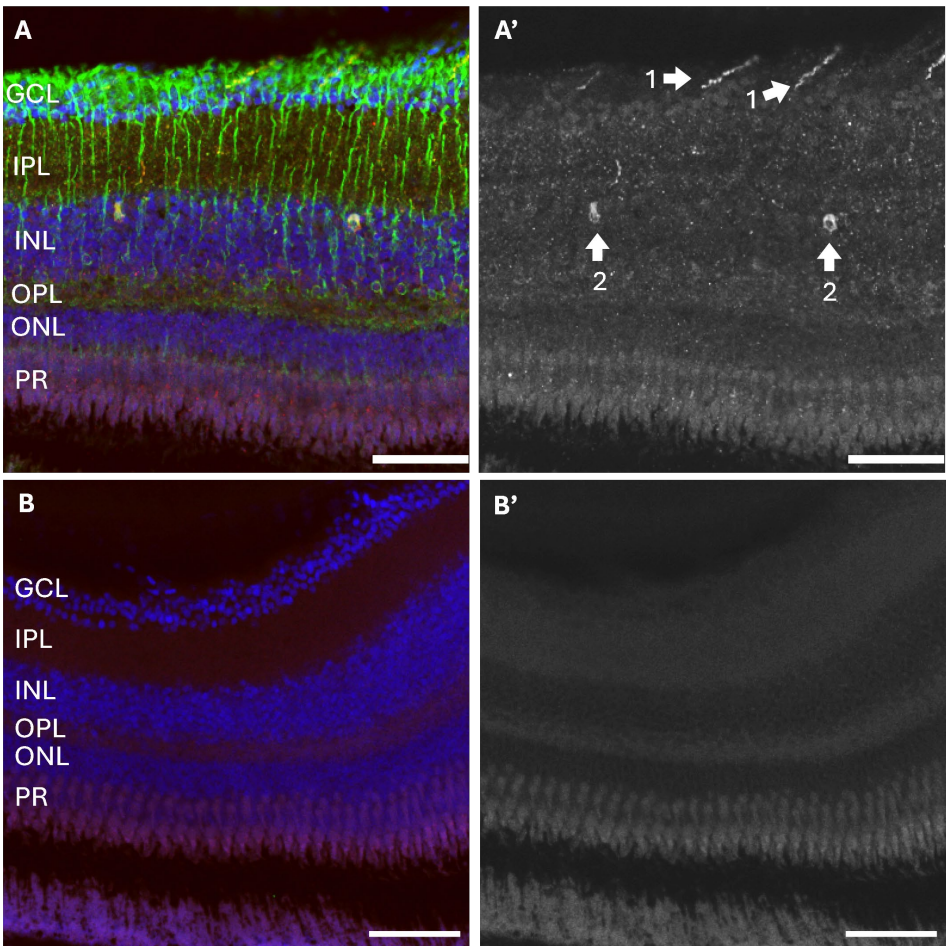

Figure 12. Retina from a juvenile wild-type zebrafish (*Danio rerio*) head cut into 20 µm thick coronal sections and labelled with pas350 diluted 1:500 (red, anti-*opn4m1, opn4m2,* and *opn4m3*; with Alexa 555 diluted 1:500), GFAP diluted 1:1600 (green, glial cell marker; with Alexa 488 diluted 1:500), and DAPI (blue, nuclear stain). (A) Labelled retina showing all channels imaged. (A') Labelled retina showing only the 561 nm channel (red) with white arrows showing examples of pas350 labelling in the retinal ganglion cell layer (1) and inner nuclear layer (2). (B) No primary control showing all channels. (B') No primary control showing only the 561 nm channel. Brightness was increased by 20% using PowerPoint's picture format corrections feature for all four images. Abbreviations: GCL = ganglion cell layer, INL = inner nuclear layer, IPL = inner plexiform layer, ONL = outer nuclear layer, OPN = outer plexiform layer, PR = photoreceptor layer. Scale bars = 50 µm

In two zebrafish retinas, OPN4L labelled cell bodies in the inner nuclear layer, likely amacrine cells, the base of the photoreceptors, and, at the two higher primary antibody concentrations, the edge of the retinal ganglion cell layer (Figure 13). GFAP and OPN4L labelling were more prominent at higher concentrations of primary antibody, though higher concentrations of OPN4L also increased background fluorescence.

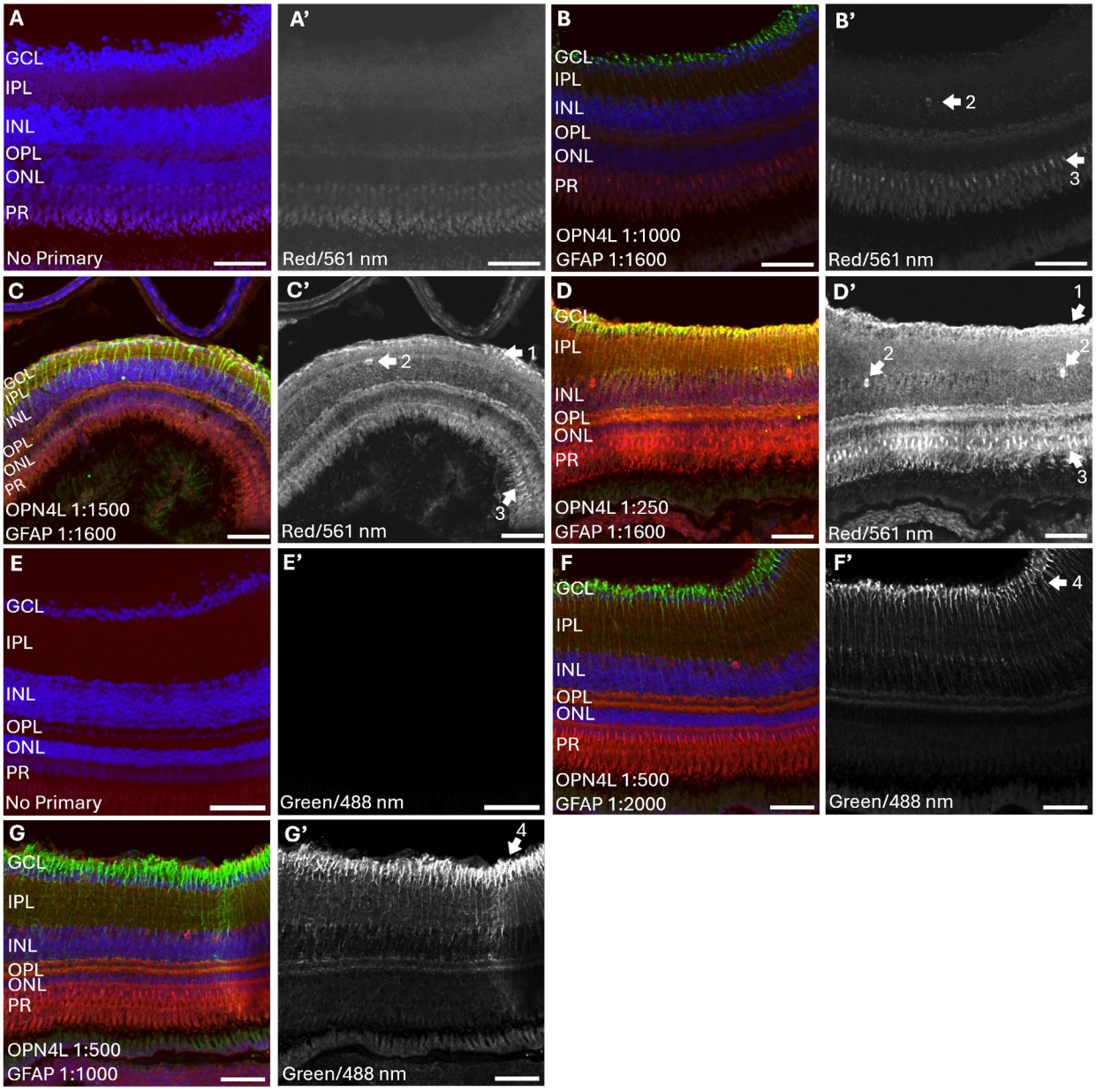

Figure 13. Two zebrafish (*Danio rerio*) retinas labelled with three dilutions of OPN4L and three dilutions of GFAP**.** (A-D) Coronal sections from one juvenile wild-type zebrafish. (next page)

(E-G) Sagittal sections of one juvenile Tg(*mylpfa*:RFP) zebrafish. Retina sections were cut to 20 µm thick and labelled with varying dilutions of OPN4L (red, anti-*opn4m2*; Alexa 555 diluted 1:500), GFAP (green, glial marker; Alexa 488 diluted 1:500), and DAPI (blue, nuclear stain). White arrows point towards examples of melanopsin labelling in (1) the ganglion cell layer, (2) inner nuclear later, (3) photoreceptors, and (4) GFAP labelling in the ganglion cell layer. (A, A') No primary antibody control showing all three channels merged (A) and only the 561 nm channel (A'). For these two panels, brightness was increased by 40% using PowerPoint. (B, B') OPN4L diluted 1:1000, GFAP diluted 1:1600 showing merged channels (B) and 561 nm channel (B'). (C, C') OPN4L diluted 1:500, GFAP diluted 1:1600 showing merged (C) and 561 nm (C') channels. (D, D') OPN4L 1:250, GFAP 1:1600 with merged (D) and 561 nm (D') channels. (E, E') No primary antibody control showing all three channels merged (E) and only the 488 nm channel (E'). (F, F') OPN4L 1:500, GFAP 1:2000, where (F) is merged and (F') is 488 nm channel. (G, G') OPN4L 1:500, GFAP 1:1000, where (G) is merged and (G') is 488 nm channel. Abbreviations: GCL = ganglion cell layer, INL = inner nuclear layer, IPL = inner plexiform layer, ONL = outer nuclear layer, OPN = outer plexiform layer, PR = photoreceptor layer. Scale bars = 50 µm.

Whole-Mount Labelled Larvae

The whole-mount zebrafish larvae (Figure 14) showed DAPI and GFAP labelling, though the labelling did not penetrate deeply into the brain (indicated by the single Z-layer images being a thin outline of labelling surrounding lack of fluorescence). OPN4L labelling appeared to be small haphazardly arranged dots, perhaps in the skin, as well as a distinct patch near the posterior end of the stomach (Figure 14 panel C"').

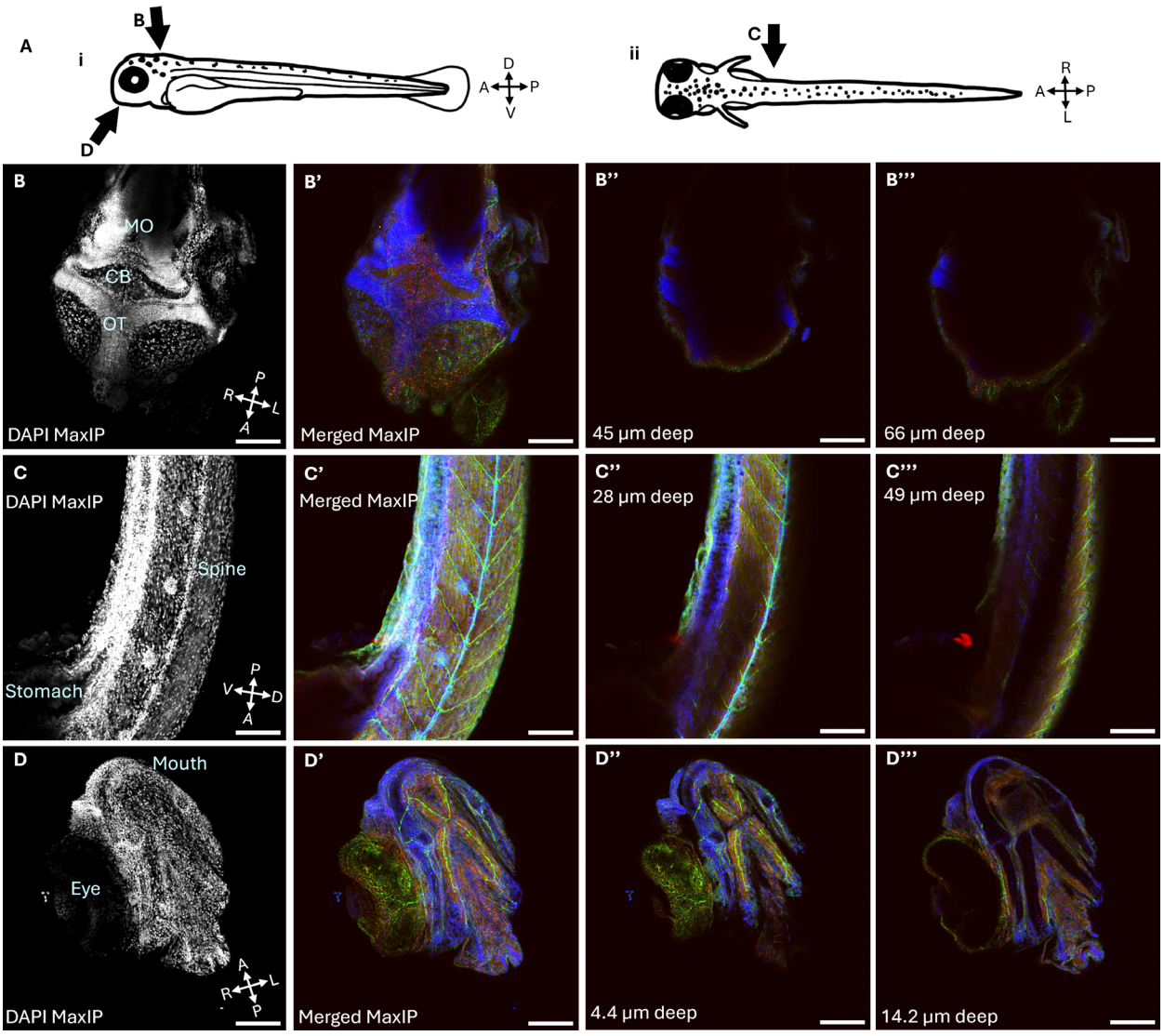

Figure 14. Whole-mount immunolabelled 10 days post fertilization (dpf) larval *casper* zebrafish (*Danio rerio*). Larvae were labelled with a nuclear stain (DAPI, blue), glial marker (anti-GFAP antibody, green, diluted 1:1600; with Alexa 488 diluted 1:500), and OPN4L antibody (anti-*opn4m2,* red, diluted 1:500, with Alexa 555 diluted 1:1000). (A) Sketches of approximately 3 dpf wild-type larval zebrafish from a side/sagittal (i) view and top-down/horizontal (ii) view with arrows pointing towards the direction images B-D are looking towards. (B-B''') Image of the top of the head. (C-C''') Image of the side of the body. (D-D''') Image of the underside of the head. Panels (B, C, D) are a maximum intensity projection of DAPI, panels (B', C', D') show maximum intensity projections with all three channels merged, panels (B'', C'', D'') show a channels-merged image of a more superficial z-layer, and (continued on the next page)

panels (B’’’, C’’’, D’’’) show a channels-merged image of a deeper z-layer. Indicated depths are approximate. Abbreviations: A = anterior, CB = cerebellum, D = dorsal, L = left, OT = optic tectum, MaxIP = maximum intensity projection, MO = medulla oblongata, P = posterior, R = right, V = ventral. Scale bars = 100 µm.

Discussion

My Honours work shows novel observations of melanopsin proteins in the zebrafish brain, which can direct light sensitivity experiments in zebrafish to focus on these brain regions and cells. My results show differences in melanopsin expression in zebrafish and sablefish, as well as differences between two antibodies for zebrafish melanopsins. Additionally, this is the first instance of using Invitrogen’s zebrafish OPN4L antibody in a publication to date.

Antibody Specificity

From the multiple sequence alignment of melanopsins (Figure 1), it appears that OPN4L will bind zebrafish *opn4m2* perfectly, with some matches to one end of the sequence for most of the melanopsins. The OPN4L’s immunogen sequence appears to match nearly as well to zebrafish *opn4m1* and *opn4m3* as sablefish melanopsins. Since there appears to be some OPN4L labelling in sablefish, either it is nonspecific binding (*i.e.*, not binding *opn4m2*) of the primary antibody, or OPN4L is able to bind melanopsins with more mismatches than I expected. In the latter case, OPN4L might also be able to bind the other zebrafish *opn4m*s. Given the lack of other proteins appearing as results to the default and lenient BLAST searches in various databases (Appendix A), it is unlikely OPN4L binds anything in zebrafish other than melanopsin. Peptide conjugate antibodies are designed by combining a specific peptide sequence (which I have referred to as “immunogen sequence” or “antigen sequence”) with another protein, such as keyhole limpet hemocyanin (KLH) as was for OPN4L and pas350, to add size to help the peptides work as immunogens (Lee *et al.*, 2016). Therefore, if zebrafish produce a protein similar to KLH, an antibody designed against a peptide conjugated to KLH might also bind that protein. While there was a match to a keyhole limpet hemocyanin (part of the whole antigen) in zebrafish, the match was imperfect and to an intergenic DNA sequence. For this match to be a source of nonspecific binding, this DNA would need to be an unannotated protein-coding gene in

the one reading frame that would create a protein with the same or similar enough sequence, which is unlikely. A caveat to the sequence searching is that antibodies do not act like DNA primers, they bind to 3D structures with charges and other properties. Whether the 3D structure of the small region of zebrafish *opn4m2* conjugated to KLH is a similar match to other melanopsins is difficult to tell this way. Similarly, whether the differing two mismatches between pas350 and the three zebrafish *opn4m*s leads to a bias in antibody binding is not clear based off the sequences alone. While the manufacturer validated the antibody with a western blot of zebrafish muscle lysate, further validation and control steps are needed to confirm the antibody's specificity (Saper, 2005). Some tests that could be done include western blots against isolated proteins, testing on cell cultures with and without the protein of interest, and incubating the primary antibody with antigen peptides before labelling, and deactivating the primary antibody through heat treatment before labelling (Saper, 2005; Jager and Vaegter, 2016). The best specificity test would be immunolabelling sections from zebrafish lacking the protein of interest (*e.g*., *opn4m2* knockouts), as this would reveal nonspecific binding in the tissue of interest (Saper, 2005; Dr. Bob Chow personal communication).

OPN4L Labelling in Juvenile and Adult Zebrafish

In the zebrafish retina (Figure 13), OPN4L labelled a subset of the cells labelled by pas350 in the retina (Davies *et al*., 2011; Barnes, 2022; Mokariasl, 2024). This is consistent with OPN4L's antigen sequence matching one of the three melanopsins that pas350 labels (Figures 1 and 2), as it should label the same cells, but might not label all of them. This demonstrates the OPN4L antibody seems to specifically label melanopsin, although, as mentioned earlier, additional tests to confirm the antibody's specificity would increase confidence in the antibody.

The optic tectum consists of layers of connected tectal neurons (Forster *et al*., 2020), afferents from retinal ganglion cells (RGCs) projecting to up to 10 distinct layers in the superficial white and grey zone (SWGZ) and central zone (CZ) (Xiao *et al*., 2005; Nevin *et al*., 2008; Robles *et al*., 2013; Kolsch *et al*., 2021), and connections to the torus longitudinalis (TL) in the SWGZ and CZ (Folgueira *et al*., 2020). In the SWGZ, the cells with OPN4L labelling are difficult to determine due to the diffuse labelling (Figure 4 panels E and E'). The melanopsin labelling in the SWGZ overlaps with everything, including GFAP labelling, so it is unclear whether the overlap is due to both proteins being present in the same cell or present in separate

cells that are on top of or under one another. The line of labelling in the central zone appears to have some structure but is difficult to identify as it does not overlap with DAPI or GFAP (Figures 4, 5, and 6). GFAP does not label all glia (Than-Trong and Bally-Cuif, 2015), and it was somewhat faint in this study, so I looked at other studies' glial labelling with GFAP and BLBP to check if there might be missing co-labelling. The GFAP and BLBP labelling still does not match the line, instead showing labelling in the periventricular grey zone and vertical lines projecting from the periventricular grey zone to the SWGZ (Than-Trong and Bally-Cuif, 2015; Lindsey *et al*., 2019; Shimizu and Kawasaki, 2021). Therefore, if the line of melanopsin labelling is either in neurons, or in a glial cell type that is not characterized by either of these markers. The line appears too large to be a single axon or synapse but could be a bundle of axons (Dr. Kerry Delaney, personal communication). It appears similar to synaptic layers labelled with nestin in Corbo *et al*. (2012)'s Figure 8. Some of the tectal neurons (Forster *et al*., 2020) and connections to and from the TL (Folgueira *et al*., 2020) have projections going horizontally across a layer. If those tectal or TL-associated neurons were expressing melanopsin only in certain projections, it could result in a similar appearance. Additionally, some RGCs have been shown to express melanopsin (Kolsch *et al*., 2021), and RGCs project to numerous layers within the SWGZ and CZ of the optic tectum (Robles *et al*., 2013), so the line might be bundles of RGC axons. I tried to look for co-labelling with RGCs through labelling the brain of a Tg(*isl2b*:QF2,QUAS:loxP-mCherry-loxP-memGCaMP8m) fish (mCherry expressed in retinal ganglion cells) (Figure 8). While the sections had poor histology, there appears to be labelling in the SWGZ with OPN4L as seen in the other samples, and in the SWGZ and CZ with anti-dsRed as expected for RGC axons. So, pursuing this co-labeling with more samples is worthwhile.

Labelling in the optic tectum of 3 month old wild-type zebrafish (Figures 4 and 5) was more visible than 6 month old *casper* zebrafish (Figure 7), which might have been due to differences in gene expression from age (Arslan-Ergul and Adams, 2014) or the transparent nature of *casper* zebrafish (White *et al*., 2008). At a higher magnification (Figure 6), there are small specks of OPN4L labelling throughout the brain, even at a 1:10,000 dilution where the line was only discernable in the maximum intensity projection image. Determining whether the small specks are labelling or an artefact of the primary antibody will take some testing, such as the additional controls mentioned above, or perhaps faster centrifuging to remove any clumps from the antibody and PBS mixture.

The potential function of *opn4m2* in the optic tectum depends on the cell types expressing melanopsin. It is possible that the intrinsically photosensitive RGCs (ipRGCs) are expressing melanopsin for use in the eye and it just happens to end up a long way away in the brain too, however that would be a large amount of extra protein to create and place in the membrane to put somewhere it is not used. Perhaps the ipRGCs are using this to compare brightnesses or help integrate light over time and over a long distance. If melanopsin is in the optic tectum or torus longitudinalis, perhaps it is sensing light as part of the overall peripheral tissue light sensing and circadian entrainment (Davies *et al*., 2015; Steindal and Whitmore, 2020), or perhaps it is part of tuning and processing visual information, in which both brain regions are involved (Forster *et al*., 2020; Baier and Wullimann, 2021;Tesmer *et al*., 2022; Baier and Scott, 2024). Additionally, it is possible that melanopsin is serving a non-light-sensing role (Kramm *et al*., 1993; Feuda *et al*., 2022). Therefore, future experiments will be needed to determine whether those cells are light sensitive, whether melanopsin contributes to that light sensitivity, and what role melanopsin is playing.

The two distinct cells labelled in Figure 4 panels G and G' are likely in the paraventricular organ (PVO) (Kenny *et al*., 2021) or posterior tuberculum nucleus (PTN) (Mueller, 2012) and appear to be large neurons, possibly neurosecretory (Dr. Kerry Delaney, personal communication), or a bundle of multiple cells as the DAPI labelling looks different than in the PGZ (Figure 4 panel H). Note, the PVO and PTN are parts of the posterior tuberculum (PT) (Muller, 2012). I only have one clear image of these cells as the rest of the sections that had a similar brain region were too damaged (*e.g*., Figure 3 panels G and H), though some of the damaged and labelled sections appear to have spots of fluorescence that might be these OPN4L labelled PVO cells (data not shown). Nearby brain regions have been shown to express opsins. Numerous opsins have been identified in the teleost thalamus (Hang *et al*., 2016), which is dorsal to my PVO labelling. Through *in-situ* hybridization, *opn4m* transcripts were found in the Atlantic salmon dorsal thalamus and hypothalamus's nucleus lateralis tuberis, and *opn4x* transcripts were observed in the supraoptic/chiasmatic nucleus and left habenula (Sandbakken *et al*., 2012). Davies *et al*. (2015) observed transcripts of a opsins, such as *opn7d* and *opn8b* in two nuclei in the hypothalamus, the caudal nucleus and dorsal nucleus (see Davies *et al*. (2015) Figure 6), however the sections appear more posterior to the one with the OPN4L PVO labelled cells. Studies also used various markers within the PVO or PT that are promising for future co-

labelling studies. Hiraki-Kajiyama *et al.* (2024) used *in situ* hybridization to characterize the transcripts of neuropeptides across the adult zebrafish brain, some of which appear to be in a similar area as the PVO labelling I found, such as *ccka*, *crhb*, *npvf*, *pdyn*, *penka*, *penkb*, *pomcb*, *gad* mix, and *vglut* mix (see Hiraki-Kajiyama *et al*., 2024's Figure 14). Kaslin *et al.* (2004) used *in situ* hybridization and immunolabelling to explore the orexin/hypocretin system and found large neurons labelled with tyrosine hydroxylase (TH) and 5-HT near the anterior PVO associated with ORX labelled neurons and the medial forebrain bundle (see Kaslin *et al*. (2004)'s Figure 3 panel L). The neurons identified by Kaslin *et al.* (2004) seem to have a similar cell body shape and direction of projections (dorsal to ventral) as the OPN4L-labelled PVO cells I found, indicating co-labelling for TH and 5-HT might help identify or rule out these as options for the OPN4L labelled PVO cells. Rink and Wullimann (2001) characterized the zebrafish dopaminergic system through immunolabelling for tyrosine hydroxylase (TH) to locate catecholaminergic neurons. Rink and Wullimann (2001) identified three types of catecholaminergic neurons in the posterior tuberculum, of which type 2 are large pear-shaped cells adjacent to the periventricular nucleus of the posterior tuberculum that seem similar to the OPN4L PVO cells. Searching the Web of Science for studies that Cite Rink and Wullimann (2001) and further discuss "pear" cells does not take this much further. One of those studies demonstrated lack of *Nr4a2* expression in the pear-shaped neurons (Chen *et al*., 2013). The other study characterized the *ETvmat2*:GFP transgenic zebrafish finding GFP expression in the large pear-shaped TH neurons and observed a reduction of these neurons after exposing the larvae to an environmental toxin, 1-methyl-4-phenyl-1,2,3,6-tetrahydropyridine (MPTP) (Wen *et al*., 2008). Searching the same set of papers for ones that mention "posterior tuberculum" gives a variety of papers, including ones characterizing dopaminergic systems in other fish species.

Given the widespread mRNA labelling of *opn4m2* in the zebrafish brain (Dekens *et al*., 2022), I was expecting to see more labelling with OPN4L. However, it makes sense that the optic tectum would be the most distinct given the diversity of opsin mRNA in the periventricular grey zone (Davies *et al*., 2015). There are a few explanations for this discrepancy. Perhaps not all the mRNA is transcribed to proteins, or the proteins are degraded quickly (Buccitelli and Selbach, 2020). Melanopsin expression is impacted by photoperiod (Matos-Cruz *et al*., 2011) and temperature (Sua-Cespedes *et al*., 2025), so there may have been differences in the conditions that led to differing amounts of melanopsin in the brains. The age and sex of zebrafish also

impact gene expression (Arslan-Ergul and Adams, 2014) and may have differed between Dekens *et al*. (2022)'s *in-situ* hybridizations and this study. However, from delving into the supplemental material from Arslan-Ergul and Adams (2014) study, it does not seem that *opn4m2* gene expression changes with age or sex, so either a post-transcriptional step changes or this is not a factor. Additionally, the protocol may not be fully optimized as the GFAP labelling seems relatively dim compared to other publications (*e.g.*, Than-Trong and Bally-Cuif, 2015). Perhaps the brains were fixed for too long as aldehyde reactions lead to higher background fluorescence (Willingham 1983; Castillo *et al*, 1989 referenced in Sun *et al*., 2017), and even though PFA is regarded as a less background fluorescence inducing fixative (Pilchova *et al*., 2025), there is still room for improvement, such as additional steps or other fixatives (Clancy and Cauller, 1998; Teng *et al*., 2025).

Other OPN4L Labelling

There was not much labelling with OPN4L in the juvenile sablefish brain (Figure 11). This is contrary to the zebrafish results and prior work with pas350 in sablefish (Barnes, 2022; Mokariasl, 2024). OPN4L appears to label blood vessels and spots that tend to be over blood vessels, though I am uncertain if the spots are labelling or antibodies pooling in indentations in the tissue. This might be due to the large number of mismatches in OPN4L's antigen sequence and the sablefish melanopsin proteins (Figure 1). OPN4L labelling the blood vessels was unexpected given the results with OPN4L in zebrafish and pas350 in sablefish (Barnes, 2022; Mokariasl, 2024). These blood vessels might nonspecifically attract antibodies (Dr. Niloufar Mokariasl, personal communication) or might have melanopsin as there is evidence for melanopsin in mouse blood vessels involved in vasorelaxation (Sikka *et al*., 2014).

Whole-mount immunolabelling of *casper* zebrafish larvae showed that antibodies can penetrate the larvae without the need for sectioning but did not penetrate deeply into the brain (Figure 14). The DAPI labelling of the brain looks as expected from comparison with the Z Brain Atlas (Randlett *et al*., 2015), however, only the outer edges are visible in deeper layers (as the edges are less deep than the inner portion), indicating that it did not penetrate all the way into the tissue, especially for the brain. While there was no control, the GFAP labelling looks distinct and matches the known presence of radial glia in the brain, muller glia in the eye, and glia projecting from the spine (Than-Trong and Bally-Cuif, 2015). OPN4L labelling appeared as speckles

throughout the maximum intensity projection images. The speckling may indicate presence of melanopsin proteins in the skin as there is evidence for melanopsin in the skin of *Xenopus* and chicken embryos (Bellingham *et al*., 2006), and melanopsin mRNA in zebrafish skin (Davies *et al*., 2015). There was also a distinct blob of melanopsin labelling near the stomach region (Figure 14 panel C”’) which is consistent with observations of light reactivity in cultured zebrafish gut and liver cells (Davies *et al*., 2015). I did not investigate this labelling further as I would need a control for comparison and would like to try some variations of methodology (*e.g.*, significantly longer antibody incubations, permeabilization with triton, exposing the brain) to allow the antibody to penetrate deeper.

pas350 Labelling in Zebrafish

The zebrafish retina labelled with pas350 (Figure 12) looks similar to prior work done with pas350 in zebrafish (Davies *et al*., 2011) and sablefish (Mokariasl, 2024). pas350 labelling is present in cells previously shown to have melanopsin, but not in all the cells shown to have melanopsin, perhaps due to the protocol needing further optimization or the antibody being at least 15 years old. This indicates that the labelling in other regions can be considered presence of *opn4m*s, however lack of labelling does not necessarily mean lack of *opn4m*s. For this discussion, I mainly consider the pas350 labelling and lack of labelling as seen in the samples.

In the zebrafish brain, pas350 labelling (Figures 9 and 10) looks remarkably different from the OPN4L labelling, showing numerous faint dots, many of which overlap with DAPI, as well as pas350 overlapping with GFAP in the torus longitudinalis (TL). This is unexpected as OPN4L should label a subset of the proteins that pas350 does, yet they do not overlap at all. However, pas350 is not a perfect match to the three *opn4m*s (Figure 2) and, from the labelling in the retina, might only show a subset of the labelling it should. Therefore, while unexpected, differing labelling between the two antibodies is still a reasonable outcome.

In the optic tectum, the nuclei labelled by pas350 are likely either superficial interneurons in the optic tectum or a type of glia not clearly labelled by GFAP, such as microglia (Barber *et al*., 2025) (Figure 9 panels A and B). Retinal ganglion cell bodies would be in the retina, projections from the TL would have cell bodies in the TL, it does not match a neat line of oval nuclei in a capillary (fish red blood cells have nuclei (Glomski *et al*., 1992)), and most of the neurons in the optic tectum have cell bodies in the periventricular grey zone (PGZ).

Outside of the optic tectum, pas350 appears to be in numerous cell bodies (Figure 10), as well as glia in the TL (Figure 9 panels C and D). Because the TL does not receive afferents from the retina (Folgueira *et al*., 2020; Baier and Scott, 2024), this supports the brain itself expressing melanopsin, rather than afferents of melanopsin expressing ipRGCs (Raja *et al*., 2023).

pas350 labelling in the zebrafish brain is also remarkably different from labelling in the sablefish brain (Barnes, 2022; Mokariasl, 2024), however the sablefish also showed evidence for co-labelling with GFAP (though in the optic tectum instead of the TL). Given the different life histories of sablefish (marine, deep sea) and zebrafish (freshwater, diurnal), and that the two species diverged around 224 million years ago (MYA) (Kumar *et al*., 2017), it is reasonable that they would have different localizations of melanopsin proteins. To put this in scale, sablefish and zebrafish diverged longer ago than humans from mice (84 MYA), dogs (94 MYA), and platypus (180 MYA), but more recently than humans and chickens (319 MYA) (Kumar *et al*., 2017).

Use of Two Melanopsin Antibodies

The combination of a general and specific melanopsin antibody reveals more information about the antibodies' labelling and melanopsin expression. OPN4L should label *opn4m2* while pas350 should label *opn4m1*, *opn4m2*, and *opn4m3*. Therefore, wherever there is *opn4m2* labelling one would expect it to be observed when using both OPN4L labelling and pas350 labelling. In the retina, OPN4L (Figure 13) labels a subset of the cells pas350 does (Figure 12, and Davies *et al*., 2011), suggesting those cells, such as photoreceptors, amacrine cells, and retinal ganglion cells, have *opn4m2* (we cannot rule out that they also have *opn4m1* or *opn4m3*). On the flip side, where there is pas350 labelling that does not show up with OPN4L indicates the melanopsin in those cells is *opn4m1*, *opn4m3*, or both, such as in horizontal cells. However, the brain is a different story as the OPN4L and pas350 labelling do not overlap. Therefore, the pas350 unique labelling in the brain is likely *opn4m1*, *opn4m3*, or both. As mentioned above, this unexpected result could be due to antibody binding biases. This may show up more prominently in the brain due to the need for protocol adjustments, such as shorter fixation duration to reduce background fluorescence, or antigen retrieval steps to un-crosslink some of the proteins. If this is true, protocol optimization could potentially reveal more pas350 labelling that overlaps with OPN4L. Testing the affinity of pas350 to each of the *opn4m*s could also reveal binding biases.

Conclusion

Melanopsin proteins are expressed in the zebrafish optic tectum. *opn4m2* is expressed diffusely in the superficial white and grey zone, a distinct layer of the central zone, and large neurons in the paraventricular organ. Either or both of *opn4m1* and *opn4m3* are expressed in superficial cell bodies in the optic tectum, cell bodies in the torus lateralis, cell bodies in the inferior lobe, and overlapping with glial labelling in the torus longitudinalis. Additionally, zebrafish and sablefish show different melanopsin labelling. The presence of melanopsin in cells bodies and glia in the brain supports the hypothesis that more regions of the brain can intrinsically sense light than just the pineal gland. This knowledge can direct future studies localizing melanopsin proteins to specific cells and guide the design of experiments to test for intrinsic light sensitivity across the zebrafish brain.

References

Andrabi, M., B. A. Upton, R. A. Lang, and S. Vemaraju. 2023. An expanding role for nonvisual opsins in extraocular light sensing physiology. *Annual Review of Vision Science* **9**: 245 - 267. doi: 10.1146/annurev-vision-100820-094018

Antinucci, P., and Hindges, R. 2016. A crystal-clear zebrafish for *in vivo* imaging. *Scientific Reports* **6**: 29490. doi: 10.1038/srep29490

Arslan-Ergul, A., and M. M. Adams. 2014. Gene expression changes in aging zebrafish (*Danio rerio*) brains are sexually dimorphic. *BMC Neuroscience* **15**: 29. doi: 10.1186/1471-2202-15-29

Baier, H., and E. K. Scott. 2024. The visual systems of zebrafish. *Annual Review of Neuroscience* **47**: 255-276. doi: 10.1146/annurev-neuro-111020-104854

Baier, H., and M. F. Wullimann. 2021. Anatomy and function of retinorecipient arborization fields in zebrafish. *The Journal of Comparative Neurology* **529**: 3454-3476. doi: 10.1002/cne.25204

Barber, H. M., C. G. Robbins, Z. Cutler, R. I. Brown, L. E. Jung, I. Werkman, and S. Kucenas. 2025. Radial astroglia cooperate with microglia to clear neuronal cell bodies during zebrafish optic tectum development. *Cell Reports* **44**: 116509. doi: 10.1016/j.celrep.2025.116509

Barnes, H. 2022. A deep dive into the sablefish (*Anoplopoma fimbria*) opsin repertoire: insight into melanopsin expression, localization and function in an unlikely demersal model. M.Sc. thesis, University of Victoria, Victoria.

Beaudry, F. E. G., T. W. Iwanicki, B. R. Z. Mariluz, S. Darnet, H. Brinkmann, P. Schneider, and J. S. Taylor. 2017. The non-visual opsins: Eighteen in the ancestor of vertebrates, astonishing increase in ray-finned fish, and loss in amniotes. *Journal of Experimental Zoology (Molecular and Developmental Evolution)* **328**: 685-386. doi: 10.1002/jez.b.22773

Bellingham, J., D. Whitmore, A. R. Philp, D. J. Wells, and R. G. Foster. 2002. Zebrafish melanopsin: isolation, tissue localisation and phylogenetic position. *Molecular Brain Research* **107**: 128-136. doi: 10.1016/s0169-328x(02)00454-0

Bellingham, J., S. S. Chaurasia, Z. Melyan, C. Liu, M. A. Cameron, E. E. Tarttelin, P. M. Iuvone, M. W. Hankins, G. Tosini, and R. J. Lucas. 2006. Evolution of melanopsin photoreceptors: Discovery and characterization of a new melanopsin in nonmammalian vertebrates. *PLoS Biology* **4**: e254. doi: 10.1371/journal.pbio.0040254

Bernardos, R. L., and P. A. Raymond. 2006. GFAP transgenic zebrafish. *Gene Expression Patterns* **6**: 1007-1013. doi: 10.1016/j.modgep.2006.04.006

Bertolesi, G. E., K. Atkinson-Leadbeater, E. M. Mackey, Y. N. Song, B. Heyne, and S. McFarlane. 2020. The regulation of skin pigmentation in response to environmental light by pineal type II opsins and skin melanophore melatonin receptors. *Journal of Photochemistry and Photobiology, B: Biology* **212**: 112024. doi: 10.1016/j.jphotobiol.2020.112024

Borges, R., W. E. Johnson, S. J. O'Brien, C. Gomes, C. P. Heesy, and A. Antunes. 2018. Adaptive genomic evolution of opsins reveals that early mammals flourished in nocturnal environments. *BMC Genomics* **19**: 121. doi: 10.1186/s12864-017-4417-8

Brown, C. M. 2007. Fluorescence microscopy - avoiding the pitfalls. *Journal of Cell Science* **120**: 1703-1705. doi: 10.1242/jcs.03433

Buccitelli, C., and M. Selbach. 2020. mRNAs, proteins and the emerging principles of gene expression control. *Nature Reviews Genetics* **21**: 630-644. doi: 10.1038/s41576-020-0258-4

Castillo, P. D., A. R. Llorente, and J. C. Stockert. 1989. Influence of fixation, exciting light, and section thickness on the primary fluorescence of samples for microfluorometric analysis. *Basic and Applied Histochemistry* 33: 251-7. PMID: 2684138.

Chen, S., G. R. Luo, T. Li, and T. X. Liu. 2013. Correlation of *Nr4a2* expression with the neuron progenitors in adult zebrafish brain. *Journal of Molecular Neuroscience* **51**: 719-723. doi: 10.1007/s12031-013-0054-0

Clancy, B., and L. J. Cauller. 1998. Reduction of background autofluorescence in brain sections following immersion in sodium borohydride. *Journal of Neuroscience Methods* **83**: 97-102. doi: 10.1016/s0165-0270(98)00066-1

Cooper, A. H., S. N. Archer, and M. O. Parker. 2025. Shedding light on the functional significance of opsins: Insights from fish. *Neuroscience and Biobehavioral Reviews* **176**: 106305. doi: 10.1016/j.neubiorev.2025.106305

Corbo, C. P., N. A. Othman, M. C. Gutkin, A. D. C. Alonso, and Z. L. Fulop. 2012. Use of different morphological techniques to analyze the cellular composition of the adult zebrafish optic tectum. *Microscopy Research and Technique* **75**: 325-333. doi: 10.1002/jemt.21061

Davies, W. I. L., L. Zheng, S. Hughes, T. K. Tamai, M. Turton, S. Halford, R. G. Foster, D. Whitmore, and M. W. Hankins. 2011. Functional diversity of melanopsins and their global expression in teleost retina. *Cellular and Molecular Life Sciences* **68**: 4115-4132. doi: 10.1007/s00018-011-0785-4

Davies, W. I. L., T. K. Tamai, L. Zheng, J. K. Fu, J. Rihel, R. G. Foster, D. Whitmore, and M. W. Hankins. 2015. An extended family of novel vertebrate photopigments is widely expressed and displays a diversity of function. *Genome Research* **25**: 1666-1679. doi: 10.1101/gr.189886.115

Dekens, M. P. S., B. M. Fontinha, M. Gallach, S. Pflugler, and K. Tessmar-Raible. 2022. Melanopsin elevates locomotor activity during the wake state of the diurnal zebrafish. *EMBO reports* **23**: e51528. doi: 10.15252/embr.202051528

Drivenes, O., A. M. Soviknes, L. O. E. Ebbesson, A. Fjose, H. -C. Seo, and J. V. Helvik. 2003. Isolation and characterization of two teleost melanopsin genes and their differential expression within the inner retina and brain. *The Journal of Comparative Neurology* **456**: 84-93. doi: 10.1002/cne.10523

Eilertsen, M., O. Drivenes, R. B. Evardsen, C. A. Bradley, L. O. E. Ebbesson, and J. V. Helvik. 2014. Exorhodopsin and melanopsin systems in the pineal complex and brain at early developmental stages of Atlantic halibut (*Hippoglossus hippoglossus*). *The Journal of Comparative Neurology* **522**: 4003-4022. doi: 10.1002/cne.23652

Ekstrom, P., and H. Meissl. 2003. Evolution of photosensory pineal organs in new light: The fate of neuroendocrine photoreceptors. *Philosophical Transactions of the Royal Society of London. Series B, Biological Sciences* **358**: 1679-1700. doi: 10.1098/rstb.2003.1303

Fernald, R. D. 2000. Evolution of eyes. *Current Opinion in Neurobiology* **10**: 444-450. doi: 10.1016/S0959-4388(00)00114-8

Feuda, R., A. K. Menon, and M. C. Gopfert. 2022. Rethinking opsins. *Molecular Biology and Evolution* **39**: msac033. doi: 10.1093/molbev/msac033

Folgueira, M., S. Riva-Mendoza, N. Ferreno-Galman, A. Castro, I. H. Bianco, R. Anadon, and J. Yanez. 2020. Anatomy and connectivity of the torus longitudinalis of the adult zebrafish. *Frontiers in Neural Circuits* **14**: 8. doi: 10.3389/fncir.2020.00008

Forster, D., T. O. Helmbrecht, D. S. Mearns, L. Jordan, N. Mokayes, and H. Baier. 2020. Retinotectal circuitry of larval zebrafish is adapted to detection and pursuit of prey. *eLife* **9**: e58596. doi: 10.7554/eLife.58596

Glomski, C. A., J. Tamburlin, and M. Chainani. 1992. The phylogenetic odyssey of the erythrocyte. III. Fish, the lower vertebrate experience. *Histology and Histopathology* **7**: 501-528.

Gyoja, F., S. Keita, T. Yamashita, and T. G. Kusakabe. 2025. An extensive survey of vertebrate-specific, nonvisual opsins identifies a novel subfamily, Q113-bistable opsin. *Genome Biology and Evolution* **17**: evaf032. doi: 10.1093/gbe/evaf032

Hang, C. Y., T. Kitahashi, and I. S. Parhar. 2016. Neuronal organization of deep brain opsin photoreceptors in adult teleosts. *Frontiers in Neuroanatomy* **10**: 48. doi: 10.3389/fnana.2016.00048

Hiraki-Kajiyama, T., N. Miyasaka, R. Ando, N. Wakisaka, H. Itoga, S. Onami, Y. Yoshihara. 2024. An atlas and database of neuropeptide gene expression in the adult zebrafish forebrain. *The Journal of Comparative Neurology* **532**: 325619. doi: 10.1002/cne.25619

Hoegg, S., H. Brinkmann, J. S. Taylor, and A. Meyer. 2004. Phylogenetic timing of the fish-specific genome duplication correlates with the diversification of teleost fish. *Journal of Molecular Evolution* **59**: 190-203. doi: 10.1007/s00239-004-2613-z

Jacobs, G. H. 2008. Primate color vision: A comparative perspective. *Visual Neuroscience* **25**: 619-633. doi: 10.1017/S0952523808080760

Jager, S. B., and C. B. Vaegter. 2016. Avoiding experimental bias by systematic antibody validation. *Neural Regeneration Research* **11**: 1079-1080. doi: 10.4103/1673-5374.187037

Jurisch-Yaksi, N., E. Yaksi, and C. Kizil. 2020. Radial glia in the zebrafish brain: Functional, structural, and physiological comparison with the mammalian glia. *Glia* **68**: 2451-2470. doi: 10.1002/glia.23849

Kami, C., S. Lorrain, P. Hornitschek, and C. Fankhauser. 2010. Light-regulated plant growth and development. *Current Topics in Developmental Biology* **91**: 29-66. doi: 10.1016/S0070-2153(10)91002-8

Kaslin, J., J. M. Nystedt, M. Ostergard, N. Peitsaro, and P. Panula. 2004. The orexin/hypocretin system in zebrafish is connected to the aminergic and cholinergic systems. *The Journal of Neuroscience* **24**: 2678-2689. doi: 10.1523/JNEUROSCI.4908-03.2004

Kenny, J. W., P. E. Steadman, O. Young, M. T. Shi, M. Polanco, S. Dubaishi, K. Covert, T. Mueller, and P. W. Frankland. 2021. A 3D adult zebrafish brain atlas (AZBA) for the digital age. *eLife* **10**: e69988. doi: 10.7554/eLife.69988

Kolsch, Y., J. Hahn, A. Sappington, M. Stemmer, A. M. Fernandes, T. O. Helmbrecht, S. Lele, S. Butrus, E. Laurell, I. Arnold-Ammer, K. Shekhar, J. R. Sanes, and H. Baier. 2021. Molecular classification of zebrafish retinal ganglion cells links genes to cell types to behavior. *Neuron* **109**: 645-662. doi: 10.1016/j.neuron.2020.12.003

Kramm, C. M., W. J. de Grip, and H. -W. Korf. 1993. Rod-opsin immunoreaction in the pineal organ of the pigmented mouse does not indicate the presence of a functional photopigment. *Cell and Tissue Research* **247:** 71-78. doi: 10.1007/BF00327987

Kumar, S., G. Stecher, M. Suleski, and S. B. Hedges. 2017. TimeTree: A resource for timelines, timetrees, and divergence times. *Molecular Biology and Evolution* **34**: 1812-1819. doi: 10.1093/molbev/msx116

Lee, B. -S., J. -S. Huang, L. P. Jayathilaka, J. Lee, and S. Gupta. 2016. Antibody production with synthetic peptides. Pp 24-47 in *High-resolution imaging of cellular proteins: Methods and protocols*, S. D. Schwartzbach, O. Skalli, and T. Schikorski, eds. Humana Press, New York, NY. doi: 10.1007/978-1-4939-6352-2_2

Lindsey, B. W., G. E. Aitken, J. K. Tang, M. Khabooshan, A. M. Douek, C. Vandestadt, and J. Kaslin. 2019. Midbrain tectal stem cells display diverse regenerative capacities in zebrafish. *Scientific Reports* **9**: 4420. doi: 10.1038/s41598-019-40734-z

Mason, J. C., R. J. Beamish, and G. A. McFarlane. 1983. Sexual maturity, fecundity, spawning, and early life history of sablefish (*Anoplopoma fimbria*) off the Pacific coast of Canada. *Canadian Journal of Fisheries and Aquatic Sciences* **40**: 2126-2134. doi: 10.1139/f83-247

Matos-Cruz, V., J. Blasic, B. Nickle, P. R. Robinson, S. Hattar, and M. E. Halpern. 2011. Unexpected diversity and photoperiod dependence of the zebrafish melanopsin system. *PLoS ONE* **6**: e25111. doi: 10.1371/journal.pone.0025111

Meng, J., X. Huang, C. Ren, and T. Xue. 2025. Non-image-forming functions of intrinsically photosensitive retinal ganglion cells. *Annual Review of Neuroscience* **48**: 211-229. doi: 10.1146/annurev-neuro-112723-035532

Mokariasl, N. 2024. Quantification of melanopsin gene expression during sablefish (*Anoplopoma fimbria*) development and spatial mapping of opn4m proteins on a newly established brain atlas. Ph. D. dissertation, University of Victoria, Victoria.

Moraes, M. N., L. V. M. de Assis, I. Provencio, and A. M. L. Castrucci. 2021. Opsins outside the eye and the skin: A more complex scenario than originally thought for a classical light sensor. *Cell and Tissue Research* **385**: 519-538. doi: 10.1007/s00441-021-03500-0

Mu, Y., D. V. Bennett, M. Rubinov, S. Narayan, C. -T. Yang, M. Tanimoto, B. D. Mensh, L. L. Looger, and M. B. Ahrens. 2019. Glia accumulate evidence that actions are futile and suppress unsuccessful behavior. *Cell* **178**: 27-43. doi: 10.1016/j.cell.2019.05.050

Mueller, T. 2012. What is the thalamus in zebrafish? *Frontiers in Neuroscience* **6**: 64. 10.3389/fnins.2012.00064

NCBI. 2025. Search results in the gene database for “Danio rerio opn4”. [Online]. NIG National Library of Medicine National Center for Biotechnology Information. Available: https://www.ncbi.nlm.nih.gov/ [2025, August 21].

Nevin, L. M., M. R. Taylor, and H. Baier. 2008. Hardwiring of fine synaptic layers in the zebrafish visual pathway. *Neural Development* **3**: 36. doi: 10.1186/1749-8104-3-36

Philp, A. R., J. M. Garcia-Fernandez, B. G. Soni, R. J. Lucas, J. Bellingham, and R. G. Foster. 2000. Vertebrate ancient (VA) opsin and extraretinal photoreception in the Atlantic salmon (*Salmo salar*). *The Journal of Experimental Biology* **203**: 1925-1936. doi: 10.1242/jeb.203.12.1925

Pilchova, V., A. Richter, M. Meurer, C. Schulz, and M. von Kockritz-Blickwede. 2025. The effect of chemical fixation with paraformaldehyde, glutardialdehyde or methanol on immunofluorescence staining of neutrophils and neutrophil extracellular traps. *Innate Immunity* **31**: 1-14. doi: 10.1177/17534259241307563

Provencio, I., G. Jiang, W. J. de Grip, W. P. Hayes. And M. D. Rollag. 1998. Melanopsin: An opsin in melanophores, brain, and eye. *PNAS* **95**: 340-345. doi: 10.1073/pnas.95.1.340

Purves, D., G. J. Augustine, D. Fitzpatrick D, L. C. Katz, A. -S. LaMantia, J. O. McNamara, and S. M. Williams. 2001. *Neuroscience 2nd edition*. Sinauer Associates, Sunderland (MA). Phototransduction. Available from: https://www.ncbi.nlm.nih.gov/books/NBK10806/

Raja, S., N. Milosavljevic, A. E. Allen, and M. A. Cameron. 2023. Burning the candle at both ends: Intraretinal signaling of intrinsically photosensitive retinal ganglion cells. *Frontiers in Cellular Neuroscience* **16**: 1095787. doi: h10.3389/fncel.2022.1095787

Randlett, O., C. L. Wee, E. A. Naumann, O. Nnaemeka, D. Schoppik, J. E. Fitzgerald, R. Portugues, A. M. B. Lacoste, C. Riegler, F. Engert, and A. F. Schier. 2015. Whole-brain activity mapping onto a zebrafish brain atlas. *Nature Methods* **12**: 1039-1046. doi: 10.1038/nmeth.3581

Rennison, D. J., G. L. Owens, and J. S. Taylor. 2012. Opsin gene duplication and divergence in ray-finned fish. *Molecular Phylogenetics and Evolution* **62**: 986-1008. doi: 10.1016/j.ympev.2011.11.030

Rink, E., and M. F. Wullimann. 2001. The teleostean (zebrafish) dopaminergic system ascending to the subpallium (striatum) is located in the basal diencephalon (posterior tuberculum). *Brain Research* **889**: 316-330. doi: 10.1016/S0006-8993(00)03174-7

Robles, E., A. Filosa, and H. Baier. 2013. Precise lamination of retinal axons generates multiple parallel input pathways in the tectum. *The Journal of Neuroscience* **33**: 5027-5039. doi: 10.1523/JNEUROSCI.4990-12.2013

Sandbakken, M., L. Ebbesson, S. Stefansson, and J. V. Helvik. 2012. Isolation and characterization of melanopsin photoreceptors of Atlantic salmon (*Salmo salar*). *The Journal of Comparative Neurology* **520**: 3727-3744. doi: 10.1002/cne.23125

Saper, C. B. 2005. An open letter to our readers on the use of antibodies. *The Journal of Comparative Neurology* **493**: 477-478. doi: 10.1002/cne.20839

Sato, S., and V. J. Kefalov. 2024. The retina-based visual cycle. *Annual review of vision science* **10**: 293-321. doi: 10.1146/annurev-vision-100820-083937

Shen, B., H. Wei, Y. Wen, Y. Geng, T. Yang, Z. Chen, S. Dong, Y. Gao, T. Li, L. Sun, B. Xie, W. Yan, Y. Zhang, and W. Wu. 2025. Optimized in vivo two-photon imaging reveals the essential role of the contralateral eye in functional optic nerve regeneration in zebrafish larvae. *Eye and Vision (London, England)* **12**: 34. doi: 10.1186/s40662-025-00447-z

Shi, Y., J. Hu, and T. Xue. 2025. Light, opsins, and life: mammalian photophysiological functions beyond image perception. *Neuron* **113**: in-press. doi: 10.1016/j.neuron.2025.05.025

Shimizu, Y., and T. Kawasaki. 2021. Differential regenerative capacity of the optic tectum of adult medaka and zebrafish. *Frontiers in Cell and Developmental Biology* **9**: 686755. doi: 10.3389/fcell.2021.686755

Sikka, G., G. P. Hussmann, D. Pandey, S. Cao, D. Hori, J. T. Park, J. Steppan, J. H. Kim, V. Barodka, A. C. Myers, L. Santhanam, D. Nyhan, M. K. Halushka, R. C. Koehler, S. H. Snyder, L. A. Shimoda, and D. E. Berkowitz. 2014. Melanopsin mediates light-dependent relaxation in blood vessels. *PNAS* **111**: 17977-17982. doi: 10.1073/pnas.1420258111

Spady, T. C., J. W. L. Parry, P. R. Robinson, D. M. Hunt, J. K. Bowmaker, and K. L. Carleton. 2006. Evolution of the cichlid visual palette through ontogenetic subfunctionalization of the opsin gene arrays. *Molecular Biology and Evolution* **23**: 1538-1547. doi: 10.1093/molbev/msl014

Steindal, I. A. F., and D. Whitmore. 2020. Zebrafish circadian clock entrainment and the importance of broad spectral light sensitivity. *Frontiers in Physiology* **11**: 1002. doi: 10.3389/fphys.2020.01002

Sua-Cespedes, C. D., D. D. David, J. A. Souto-Neto, G. Zanetti, M. N. Moraes, and A. M. L. Castrucci. 2025. Temperature-dependent expression of melanopsin (*opn4*) reveals a non-canonical response in adult zebrafish (*Danio rerio*). *Marine and Freshwater Behavior and Physiology* **58**: 53-63. doi: 10.1080/10236244.2025.2496143

Sun, Y., P. Ip, and A. Chakrabartty. 2017. Simple elimination of background fluorescence in formalin-fixed and human brain tissue for immunofluorescence microscopy. *Journal of Visualized Experiments* **127**: e56188. doi:10.3791/56188

Taylor, B. L., I. B. Zhulin, and M. S. Johnson. 1999. Aerotaxis and other energy-sensing behavior in bacteria. *Annual Review of Microbiology* **53**: 103-128. doi: 10.1146/annurev.micro.53.1.103

Teng, A. C. T., D. Mehangrey, A. Vandenbelt, K. Vearncombe, J. D. Callahan, P. Mistry, W. Li, C. K. Reitz, O. Hamed, M. Roche, U. Kuzmanov, J. E. Fish, S. Epelman, and A. O. Gramolini. 2025. Glyoxal is a superior fixative to formaldehyde in promoting antigenicity and structural integrity in murine cardiac tissues. *Journal of Molecular and Cellular Cardiology Plus* **12**: 100454. doi: 10.1016/j.jmccpl.2025.100454

Terakita, A. 2005. The opsins. *Genome Biology* **6**: 213. doi: 10.1186/gb-2005-6-3-213

Tesmer, A. L., N. P. Fields, and E. Robles. 2022. Input from torus longitudinalis drives binocularity and spatial summation in zebrafish optic tectum. *BMC Biology* **20**: 24. doi: 10.1186/s12915-021-01222-x

Than-Trong, E., and L. Bally-Cuif. 2015. Radial glia and neural progenitors in the adult zebrafish central nervous system. *Glia* **63**: 1406-1428. doi: 10.1002/glia.22856

Upton, B. A., N. M. Diaz, S. A. Gordon, R. N. Van Gelder, E. D. Buhr, and R. A. Lang. 2021. Evolutionary constraint on visual and nonvisual mammalian opsins. *Journal of Biological Rhythms* **36**: 109-126. doi: 10.1177/0748730421999870

Visscher, K., G. J. Brakenhoff, and T. D. Visser. 1994. Fluorescence saturation in confocal microscopy. *Journal of Microscopy* **175**: 162-165. doi: 10.1111/j.1365-2818.1994.tb03479.x

Wada, S., B. Shen, E. Kawano-Yamashita, T. Nagata, M. Hibi, S. Tamotsu, M. Koyanagi, and A. Terakita. 2018. Color opponency with a single kind of bistable opsin in the zebrafish pineal organ. *PNAS* **115**: 11310-11315. doi: 10.1073/pnas.1802592115

Wen, L., W. Wei, W. Gu, P. Huang, X. Ren, Z. Zhang, Z. Zhu, S. Lin, and B. Zhang. 2008. Visualization of monoaminergic neurons and neurotoxicity of MPTP in live transgenic zebrafish. *Developmental Biology* **314**: 84-92. doi: 10.1016/j.ydbio.2007.11.012

White, R. M., A. Sessa, C. Burke, T. Bowman, J. LeBlanc, C. Ceol, C. Bourque, M. Dovey, W. Goessling, C. E. Burns, and L. I. Zon. 2008. Transparent adult zebrafish as a tool for in vivo transplantation analysis. *Cell Stem Cell* **2**: 183 - 189. doi: 10.1016/j.stem.2007.11.002

Willingham, M. C. 1983. An alternative fixation-processing method for preembedding ultrastructural immunocytochemistry of cytoplasmic antigens. *The Journal of Histochemistry and Cytochemistry* **31**: 791-798. doi: 10.1177/31.6.6404984

Wullimann, M. F., B. Rupp, and H. Reichert. 1996. *Neuroanatomy of the zebrafish brain: A topological atlas*. Birkhauser Verlag, Basel, Switzerland.

Xiao, T., T. Roeser, W. Staub, and H. Baier. 2005. A GFP-based genetic screen reveals mutations that disrupt the architecture of the zebrafish retinotectal projection. *Development* **132**: 2955-2967. doi: 10.1242/dev.0186

Yu, Z., and R. Fischer. 2018. Light sensing and responses in fungi. *Nature Reviews Microbiology* **17**: 25-36. doi: 10.1038/s41579-018-0109-x

ZFIN. 2025. Search results for genes with the name/symbol “opn4”. [Online]. The Zebrafish Information Network. Available: https://zfin.org/ [2025, August 21].

ZFIN. 2026. Zebrafish developmental staging series. [Online]. The Zebrafish Information Network. Available: https://zfin.org/zf_info/zfbook/stages/ [2026, May 5].

Appendix

Appendix A. NCBI BLAST search results for OPN4L immunogen sequences.

This table contains unique results from NCBI BLAST using the query sequence "TIRAAGKEIRELDCGETHKVYERMQNEWKMAKVA" (the region of Danio rerio opn4m2 conjugated to the keyhole limpet protein as mentioned by ThermoFisher) in BLASTP in the nr and refseq_protein databases and TBLASTN on the core_nt and nt databases. It also contains the results for discontiguous megablast searches with keyhole limpet hemocyanin sequences (*Megathura crenulata* KLH1 Accession AJ698341.2, and KLH2 Accession AJ698342.1) as the query. For the E-value, if there were differing numbers between the two databases, either the number from nr (if in both nr and refseq_protein) or from core_nt (if in both core_nt and nt) was used for this table.

				From Description Table					From Hit Table										
Search	**Species searched**	**database**	**Subject Accession**	**Description**	**Scientific Name**	**Query Cover**	**Percent identity**	**Accession Length**	**E-value**	**Alignment length**	**mismatches**	**Gap opens**	**Query start**	**Query End**	**Subject start**	**Subject end**	**Bit score**	**% positives**	**Query/ subject frames**
blastp; default	*Danio rerio*	nr and refseq_protein	NP_840074.2	melanopsin-like [Danio rerio]	*Danio rerio*	1	100	500	8.1E-19	34	0	0	1	34	255	288	78.2	100	#N/A
blastp; default	*Danio rerio*	nr	AAL82577.1	melanopsin [Danio rerio]	*Danio rerio*	1	100	501	8.1E-19	34	0	0	1	34	255	288	78.2	100	#N/A
blastp; default	*Danio rerio*	nr and refseq_protein	XP_073773405.1	opsin 4b isoform X1 [Danio rerio]	*Danio rerio*	1	50	565	0.016	34	17	0	1	34	263	296	32	61.76	#N/A
blastp; default	*Danio rerio*	nr and refseq_protein	NP_001245153.1	opsin 4b [Danio rerio]	*Danio rerio*	1	50	565	0.016	34	17	0	1	34	263	296	32	61.76	#N/A
blastp; default	*Danio rerio*	nr and refseq_protein	XP_009304843.1	opsin 4b isoform X2 [Danio rerio]	*Danio rerio*	1	50	564	0.016	34	17	0	1	34	263	296	32	61.76	#N/A
blastp; default	*Danio rerio*	nr and refseq_protein	XP_073773406.1	opsin 4b isoform X3 [Danio rerio]	*Danio rerio*	1	50	433	0.016	34	17	0	1	34	263	296	32	61.76	#N/A
blastp; default	*Danio rerio*	nr and refseq_protein	NP_001122233.2	melanopsin-A [Danio rerio]	*Danio rerio*	0.56	52.63	593	0.037	19	9	0	16	34	284	302	30.8	89.47	#N/A
blastp; default	*Danio rerio*	nr	AAI62681.1	Opsin 4a (melanopsin) [Danio rerio]	*Danio rerio*	0.56	52.63	593	0.037	19	9	0	16	34	284	302	30.8	89.47	#N/A
blastp; default	*Danio rerio*	nr	ADN39430.1	melanopsin opn4m1 [Danio rerio]	*Danio rerio*	0.56	52.63	592	0.037	19	9	0	16	34	283	301	30.8	89.47	#N/A
blastp; default	*Danio rerio*	nr and refseq_protein	XP_073775997.1	melanopsin-A isoform X1 [Danio rerio]	*Danio rerio*	0.56	52.63	545	0.037	19	9	0	16	34	236	254	30.8	89.47	#N/A
blastp; default	*Danio rerio*	nr	AAX73256.1	mammalian-like melanopsin, partial [Danio rerio]	*Danio rerio*	0.56	52.63	357	0.037	19	9	0	16	34	211	229	30.8	89.47	#N/A
blastp; default	*Anoplopoma fimbria*	refseq_protein	XP_054483128.1	LOW QUALITY PROTEIN: melanopsin-like [Anoplopoma fimbria]	*Anoplopoma fimbria*	0.97	57.58	442	1.14 E-08	33	14	0	2	34	248	280	47.8	81.82	#N/A
blastp; default	*Anoplopoma fimbria*	refseq_protein	XP_054454330.1	melanopsin-A-like [Anoplopoma fimbria]	*Anoplopoma fimbria*	0.97	38.89	552	0.008	36	19	1	2	34	252	287	31.2	61.11	#N/A

				From Description Table					From Hit Table										
Search	**Species searched**	**database**	**Subject Accession**	**Description**	**Scientific Name**	**Query Cover**	**Percent identity**	**Accession Length**	**E-value**	**Alignment length**	**mismatches**	**Gap opens**	**Query start**	**Query End**	**Subject start**	**Subject end**	**Bit score**	**% positives**	**Query/ subject frames**
blastp; default	*Anoplopoma fimbria*	refseq_protein	XP_054456109.1	melanopsin-A [Anoplopoma fimbria]	*Anoplopoma fimbria*	0.41	71.43	560	0.008	14	4	0	21	34	293	306	31.2	100	#N/A
tblastn; default	*Danio rerio* and *Anoplopoma fimbria*	core_nt and nt	BX323807.8	Zebrafish DNA sequence from clone DKEY-154P10 in linkage group 2, complete sequence	*Danio rerio*	1	100	194313	9.75E-18	34	0	0	1	34	168834	168733	78.2	100	0/-1
tblastn; default	*Danio rerio* and *Anoplopoma fimbria*	core_nt and nt	XM_073911392.1	PREDICTED: Danio rerio PX domain containing 1a (pxdc1a), transcript variant X1, mRNA	*Danio rerio*	1	100	4616	9.84E-18	34	0	0	1	34	2304	2405	78.2	100	0/3
tblastn; default	*Danio rerio* and *Anoplopoma fimbria*	core_nt and nt	GQ925716.1	Danio rerio melanopsin opn4m2 mRNA, complete cds	*Danio rerio*	1	100	1503	9.86E-18	34	0	0	1	34	763	864	78.2	100	0/1
tblastn; default	*Danio rerio* and *Anoplopoma fimbria*	core_nt and nt	KT008429.1	Danio rerio mammalian-like melanopsin-2 (opn4m2) mRNA, complete cds	*Danio rerio*	1	100	1503	9.86E-18	34	0	0	1	34	763	864	78.2	100	0/1
tblastn; default	*Danio rerio* and *Anoplopoma fimbria*	core_nt and nt	NM_178289.3	Danio rerio opsin 4.1 (opn4.1), mRNA	*Danio rerio*	1	100	3218	9.88E-18	34	0	0	1	34	880	981	78.2	100	0/1
tblastn; default	*Danio rerio* and *Anoplopoma fimbria*	core_nt and nt	AY078161.1	Danio rerio melanopsin mRNA, complete cds	*Danio rerio*	1	100	1668	9.97E-18	34	0	0	1	34	790	891	78.2	100	0/1
tblastn; default	*Danio rerio* and *Anoplopoma fimbria*	core_nt and nt	XM_054627153.1	PREDICTED: Anoplopoma fimbria opsin 4.1 (opn4.1), mRNA	*Anoplopoma fimbria*	0.97	57.58	1423	4.91E-07	33	14	0	2	34	836	934	47.8	81.82	0/2
tblastn; default	*Danio rerio* and *Anoplopoma fimbria*	nt	CP137033.3	Danio rerio strain Tubingen chromosome 2	*Danio rerio*	1	100	63727224	5.77E-17	34	0	0	1	34	35987222	35987323	78.2	100	0/2
tblastn; default	*Danio rerio* and *Anoplopoma fimbria*	nt	OX063291.1	Danio rerio genome assembly, chromosome: 2	*Danio rerio*	1	100	63032945	5.77E-17	34	0	0	1	34	35174871	35174972	78.2	100	0/3
tblastn; default	*Danio rerio* and *Anoplopoma fimbria*	nt	LR812064.1	Danio rerio genome assembly, chromosome: 2	*Danio rerio*	1	100	59970185	5.77E-17	34	0	0	1	34	32460104	32460205	78.2	100	0/2
tblastn; default	*Danio rerio* and *Anoplopoma fimbria*	nt	CP068736.1	Danio rerio strain T5D chromosome 2	*Danio rerio*	1	100	59455749	5.77E-17	34	0	0	1	34	32811687	32811788	78.2	100	0/3
tblastn; default	*Danio rerio* and *Anoplopoma fimbria*	nt	LR812570.1	Danio rerio strain Nadia (NA) genome assembly, chromosome: 2	*Danio rerio*	1	100	59275206	5.77E-17	34	0	0	1	34	33818583	33818684	78.2	100	0/3

				From Description Table					From Hit Table										
Search	**Species searched**	**database**	**Subject Accession**	**Description**	**Scientific Name**	**Query Cover**	**Percent identity**	**Accession Length**	**E-value**	**Alignment length**	**mismatches**	**Gap opens**	**Query start**	**Query End**	**Subject start**	**Subject end**	**Bit score**	**% positives**	**Query/ subject frames**
tblastn; default	*Danio rerio* and *Anoplopoma fimbria*	nt	LR812595.1	Danio rerio genome assembly, chromosome: 2	*Danio rerio*	1	100	58067448	5.77E-17	34	0	0	1	34	32799705	32799806	78.2	100	0/3
tblastn; default	*Danio rerio* and *Anoplopoma fimbria*	nt	LR812039.1	Danio rerio genome assembly, chromosome: 2	*Danio rerio*	1	100	57662316	5.77E-17	34	0	0	1	34	31805837	31805938	78.2	100	0/2
tblastn; default	*Danio rerio* and *Anoplopoma fimbria*	nt	LR812545.1	Danio rerio strain Cooch Behar (CB) genome assembly, chromosome: 2	*Danio rerio*	1	100	54745004	5.77E-17	34	0	0	1	34	32183175	32183276	78.2	100	0/3
tblastn; default	*Anoplopoma fimbria*	nt	XM_054598355.1	PREDICTED: Anoplopoma fimbria melanopsin-A-like (LOC129090956), mRNA	*Anoplopoma fimbria*	0.97	38.89	1659	0.015	36	19	1	2	34	754	861	31.2	61.11	0/1
tblastn; default	*Anoplopoma fimbria*	nt	XM_054600134.1	PREDICTED: Anoplopoma fimbria opsin 4a (melanopsin) (opn4a), mRNA	*Anoplopoma fimbria*	0.41	71.43	1683	0.016	14	4	0	21	34	877	918	31.2	100	0/1
tblastn; lenient, whole	*Danio rerio* and *Anoplopoma fimbria*	refseq_genomes	NC_133177.1	Danio rerio strain Tuebingen ecotype United States chromosome 2, GRCz12tu	*Danio rerio*	1	100	63578853	7.17E-13	34	0	0	1	34	35815130	35815130	63.4	100	0/2
tblastn; lenient, whole	*Danio rerio* and *Anoplopoma fimbria*	refseq_genomes	NC_072451.1	Anoplopoma fimbria isolate UVic2021 breed Golden Eagle Sablefish chromosome 3, Afim_UVic_2022	*Anoplopoma fimbria*	0.97	57.58	27098089	1.99E-04	33	14	0	2	34	35815130	35815130	39.9	81.82	0/-2
tblastn; lenient, first half	*Danio rerio* and *Anoplopoma fimbria*	refseq_genomes	NC_133177.1	Danio rerio strain Tuebingen ecotype United States chromosome 2, GRCz12tu	*Danio rerio*	1	100	63578853	0.019	17	0	0	1	17	35815130	35815180	34	100	0/2
tblastn; lenient, last half	*Danio rerio* and *Anoplopoma fimbria*	refseq_genomes	NC_133177.1	Danio rerio strain Tuebingen ecotype United States chromosome 2, GRCz12tu	*Danio rerio*	1	100	63578853	0.004	17	0	0	1	17	35815181	35815231	36.1	100	0/2
discontiguous megablast; default; KLH1	*Danio rerio* and *Anoplopoma fimbria*	nt	no matches	#N/A	#N/A	#N/A	#N/A	#N/A	#N/A	#N/A	#N/A	#N/A	#N/A	#N/A	#N/A	#N/A	#N/A	#N/A	#N/A
discontiguous megablast; default; KLH1	*Danio rerio* and *Anoplopoma fimbria*	refseq_genomes	NC_133200.1	Danio rerio strain Tuebingen ecotype United States chromosome 25, GRCz12tu	*Danio rerio*	0	86.05	40454730	0.013	43	6	0	4654	4696	32249437	32249395	51.8	#N/A	#N/A
discontiguous megablast; default; KLH2	*Danio rerio* and *Anoplopoma fimbria*	nt	no matches	#N/A	#N/A	#N/A	#N/A	#N/A	#N/A	#N/A	#N/A	#N/A	#N/A	#N/A	#N/A	#N/A	#N/A	#N/A	#N/A	#N/A
discontiguous megablast; default; KLH2	*Danio rerio* and *Anoplopoma fimbria*	refseq genomes	no matches	#N/A	#N/A	#N/A	#N/A	#N/A	#N/A	#N/A	#N/A	#N/A	#N/A	#N/A	#N/A	#N/A	#N/A	#N/A	#N/A	#N/A